Volume 51 / Supplement 108 / 2022

Vasa

European Journal of Vascular Medicine

22. Unionstagung der Schweizerischen Gesellschaften für Gefässkrankheiten gemeinsam mit der Schweizerischen Gesellschaft für Ultraschall in der Medizin Sektion Gefässe

22e Congrès de l'Union des Sociétés Suisses des Maladies Vasculaires en collaboration avec la Société Suisse d'Ultrasons en Médecine Section Vaisseaux

2. – 4. November 2022 | 2 – 4 novembre 2022
Kongresshaus Zürich

Union of Vascular Societies of Switzerland
Union Schweizerischer Gesellschaften für Gefässkrankheiten
Union des Sociétés Suisses des Maladies Vasculaires
Unione delle Società Svizzere di malattie vascolari
Uniun da las Societads Svizras da malsognas vascularas
USGG / USSMV www.uvs.ch

hogrefe

Vasa

European Journal of Vascular Medicine

Volume 51 / Supplement 108 / 2022

22. Unionstagung der Schweizerischen Gesellschaften für Gefässkrankheiten gemeinsam mit der Schweizerischen Gesellschaft für Ultraschall in der Medizin Sektion Gefässe

22e Congrès de l'Union des Sociétés Suisses des Maladies Vasculaires en collaboration avec la Société Suisse d'Ultrasons en Médecine Section Vaisseaux

2. – 4. November 2022 | 2 – 4 novembre 2022
Kongresshaus Zürich

Meister ConCept GmbH
Bahnhofstrasse 55
5001 Aarau
T +41 62 836 20 90
F +41 62 836 20 97
unionstagung@meister-concept.ch

hogrefe

www.vasa-journal.eu
Article submissions:
www.editorialmanager.com/vasa

Publisher Hogrefe AG, Länggass-Strasse 76, Postfach CH-3012 Bern, Switzerland, Tel. +41 (0) 31 300 45 00, verlag@hogrefe.ch, www.hogrefe.com/ch

Subscriptions Tel. +41 (0) 31 300 45 55, zeitschriften@hogrefe.ch

Production Gerda Schotte, Tel. +41 (0) 31 300 45 78, gerda.schotte@hogrefe.ch

Frequency 6 online issues per volume

Vasa is the official organ of German Society of Angiology – Society of Vascular Medicine, Swiss Society of Angiology, Slovenian Society of Vascular Diseases , and European Society for Vascular Medicine.

Vasa is listed in Medline, Science Citation Index, Expanded (SCIE), SciSearch Current Contents/Clinical Medicine, Science Citation Index, Prous Science Integrity, Journal Citation Reports/Science Edition, Biological Abstracts, BIOSIS Previews, EMBASE, and Scopus.

Library of Congress Catalog Card Number 72-96 773

Impact Factor 2.336 (Journal Citation Reports 2021 SCI, © Clarivate Analytics 2022)

H Index 36

Prices *Subscription rates per volume:*
Libraries/Institutions: from CHF 505.– / € 427.– / US $ 490.– (Prices depend on the size of the institution and can be found can be found in our journals catalogue: hgf.io/zftkatalog)

Individuals: CHF 172.– / € 128.– / US $ 159.–

Single Issue: CHF 74.– / € 55.– / US $ 69.–

Vasa is available online only.

ISSN-L 0301-1526
ISSN 1664-2872 (online)

Themenübersicht / Aperçu des thèmes

Angiologie

FM 1.5

Percutaneous angioplasty and stenting in patients with upper extremity peripheral artery disease (PAD)

R. Fumagalli, K. Schürch, N. Kucher, S. Barco,
Presenter: R. Fumagalli (Zürich)

Objective: Upper extremity PAD is a rare manifestation of PAD mainly affecting subclavia and innominate arteries and presents with a broad spectrum of signs and symptoms. In the presence of symptoms, revascularization should be considered. If opting for an endovascular approach, stent placement seems to be better than percutaneous angioplasty (PTA) alone in terms of one-year patency. The aim of the present study is an evaluation of the characteristics and clinical course of patients with upper extremity PAD treated with a single endovascular approach.
Methods: We retrospectively analyzed all the patients treated for upper extremity PAD with angioplasty plus balloon expandable BeSmooth stent® (Bentley Innomed GmbH, Germany) placement at a university hospital between 2018 and 2022. Primary outcome was the rate of restenosis and re-occlusion of the target lesion, inclusive of the need of reintervention. Secondary outcomes included rate of arm claudicatio and subclavian steal syndrome symptoms, brachial oscillometric measurements of the blood pressure, and death. Ethic approval was obtained.
Results: 27 patients were treated with PTA and stent implantation in the subclavian artery (74%) or in the innominate artery (26%). The median age was 70 years (SD 14) and 59% were male. A total of 23 (85%) patients had a previous revascularization, including 3 (11%) at target vessel. At discharge 25 (93%) patients received antiplatelet treatment and 2 (8%) received long term xarelto vascular (2,5 mg). After a median 6 months follow-up (range 3–12) in-stent occlusion occurred in 1 (4%) patient and in-stent stenosis in 5 (19%) patients. In 2 (8%) cases, an elective revascularization was needed. 1 (4%) patient primary treated for an acute occlusion died on 10th postoperative day for septic shock. At last available follow-up no patient complained of arm claudicatio or steal syndrome symptoms, and moderate or heavy pathological oscillometric measurements normalized in all surviving patients.
Conclusion: Percutaneous catheter-based treatment with stenting for upper extremity PAD appeared to be effective and lead to durable results. Data from randomized controlled trials is urgently needed.

YI 6

Molecular atlas of the human brain vasculature across development, adulthood and disease at the single- cell level

M. Ghobrial, Presenter: M. Ghobrial (Zurich)

Objective: A broad range of brain pathologies critically relies on the vasculature, and cerebrovascular disease is a leading cause of death worldwide. However, the cellular and molecular architecture of the human brain vasculature remains poorly understood.
Methods: Here, we performed single-cell RNA sequencing of 599,215 freshly isolated endothelial, perivascular and other tissue-derived cells from 47 fetuses and adult patients to construct a molecular atlas of the developing fetal, adult control and diseased human brain vasculature.
Results: We uncover extensive molecular heterogeneity of the vasculature of healthy fetal and adult human brains and across eight vascular-dependent CNS pathologies including brain tumors and brain vascular malformations. We identify alteration of arteriovenous differentiation and reactivated fetal as well as conserved dysregulated genes/pathways in the diseased vasculature. Pathological endothelial cells display a loss of CNS-specific properties and reveal an upregulation of MHC class II molecules, indicating atypical features of CNS endothelial cells. Cell-cell interaction analyses predict numerous endothelial-to-perivascular cell ligand-receptor crosstalk including immune-related and angiogenic pathways, thereby unraveling a central role for the endothelium within brain neurovascular unit signaling networks.
Conclusion: Our single-cell brain atlas provides insight into the molecular architecture and heterogeneity of the developing, adult/control and diseased human brain vasculature and serves as a powerful reference for future studies.

YI 1

Enoxaparin for symptomatic outpatients with COVID-19: 90-day results from the randomised, open- label, parallel-group, multicentre, phase III OVID trial

D. Voci[1], A. Götschi[1], U. Held[1], R. Bingisser[2], G. Colucci[3], D. Duerschmied[4], B. Gerber[5], D. Keller[6], S. V. Konstantinides[7], F. Mach[8], M. Righini[8], T. Rosemann[6], S. Stortecky[9], N. Kucher[6], S. Barco[6], Presenter: D. Voci[1] ([1]Zürich, [2]Basel, [3]Lugano, [4]Heildelberg, [5]Bellinzona, [6]Zurich, [7]Mainz, [8]Geneva, [9]Bern)

Objective: It is unclear whether it may improve the course of COVID-19 among outpatients beyond the acute phase, including that of COVID-19-related symptoms. We present the final, 90-day results of the OVID phase III randomised controlled trial.
Methods: OVID was a randomised, open-label, parallel-group, investigator-initiated phase III superiority trial conducted at Swiss and German centres between August 2020 and January 2022. Patients with a positive test for SARS-CoV2, aged 50 years or older, with acute respiratory symptoms or body temperature >37.5 °C, and eligible for ambulatory treatment were screened. Patients were randomised to receive either enoxaparin 40 mg subcutaneously for 14 days or no thromboprophylaxis. The primary endpoint was the composite of untoward hospitalisation and all-cause death within 90 days. Secondary endpoints included major cardiovascular events within 90 days. We studied COVID-19-related symptoms in the two treatment arms over time: data was prospectively collected during follow-up telephone visits at day 3, 7, 14, 30, and 90.
Results: We randomised 475 patients at nine sites in Switzerland and Germany from August 2020 through January 2022. The final intention to treat (ITT) population consisted of 472 individuals: 234

https://doi.org/10.1024/0301-1526/a001036

in the enoxaparin arm and 238 in the control arm. Median age was 57 (Q1-Q3: 53–62), 217 (46%) patients were women. The primary efficacy outcome occurred in 11 (4.7%) patients of the enoxaparin group and in 11 (4.6%) of controls within 90 days after randomisation (adjusted relative risk 1.00; 95%CI: 0.44–2.25; Figure 1). In the enoxaparin arm, 2 (0.9%) patients had a cardiovascular event vs. 4 (1.7%) in the standard-of-care arm (relative risk 0.51; 95%CI: 0.09–2.75). The prevalence of COVID-19-related symptoms showed a declining trend over 90 days, which was similar in the two treatment arms (Figure 2). A total of 42 (17.9%) patients in the enoxaparin group and 40 (16.8%) patients in the control group had persistent respiratory symptoms (cough, rhinorrhea, expectoration, sore throat, dyspnea) at 90 days.

Conclusion: Early treatment with low-molecular-weight heparin did not improve the course of COVID-19 in adult symptomatic outpatients in terms of hospitalisations, deaths, and COVID-19-related symptoms over 90-day follow-up.

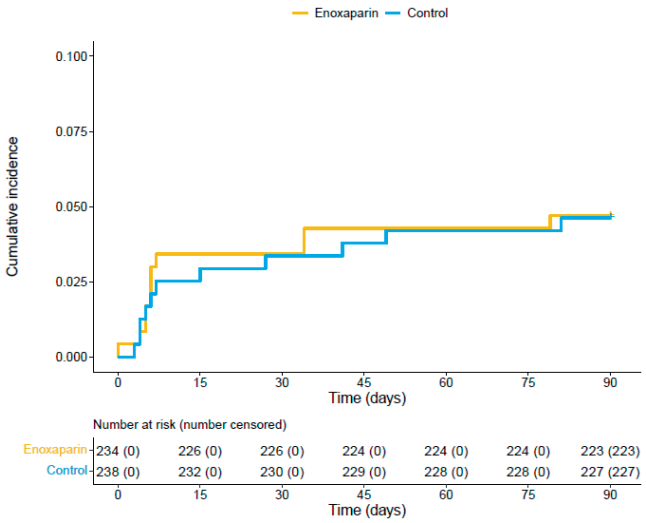

Figure 1. Cumulative incidence of the primary outcome within 90 days.

YI 2

Quality of warfarin anticoagulation in adults with short bowel syndrome on home parenteral nutrition

R. Fumagalli[1], M. Szlaszynska[1], M. Di Nisio[2], S. Barco[1],
Presenter: R. Fumagalli[1] ([1]Zürich, [2]Chieti)

Objective: Patients with short bowel syndrome and nutritional deficiency necessitate long-term home parenteral nutrition (HPN). Thromboembolic complications in patients on HPN have an annual incidence of about 12%, whereas the prevalence is at least 50%. There is no firm evidence on optimal anticoagulation for HPN patients. Vitamin K antagonists (VKA) remain the most widely used drug class in this patient group. In light of the substantial paucity of data on quality of VKA anticoagulation in adults on HPN, its safety and effectiveness are uncertain.

Methods: This retrospective cohort study included adult patients on long-term HPN managed at a university hospital (2004–2015). HPN patients on warfarin therapy were matched based on sex, age, and indication for anticoagulation to controls also on warfarin. We compared time in therapeutic range (TTR) of therapeutic-dosed warfarin treatment (INR range 2.0–3.0) between the two groups and assessed thrombotic and bleeding events. Incidence rates of were calculated as number of events/100 patient-years. Ethical approval was obtained.

Results: 12 patients on HPN and 96 control patients were included. Median follow-up time was 48 (Q1–Q3: 23–89) months for HPN patients and 30 (Q1– Q3 19–43) months for controls. Overall, median TTR calculated over the entire follow-up period of warfarin anticoagulation was 62% (Q1–Q3: 47–73) in HPN patients and 68% (Q1–Q3: 55–78) in controls. The incidence of a composite of thromboembolic, major bleeding, and anticoagulation- related death events was similar in both groups with an incidence ratio of 0.9 (95% CI: 0.2–3.0) events per 100 patient-years. Only one patient from controls died for an intracerebral hemorrhage.

Conclusion: VKA anticoagulation can be adequately managed in HPN patients and is associated to a low rate of complications.

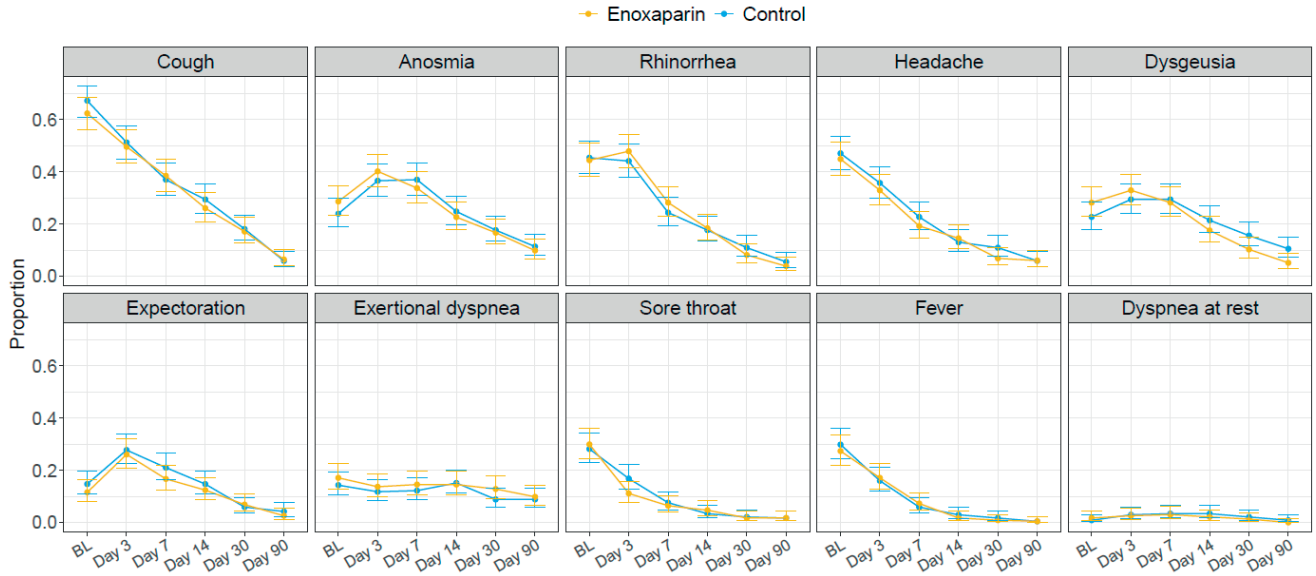

Figure 2. Trend of signs and symptoms of COVID-19 within 90 days.

YI 4

Mortality rate related to peripheral artery disease: A retrospective analysis of epidemiological data (years 2008–2019)

D. Voci[1], U. Fedeli[2], L. Valerio[3], E. Schievano[2], M. Righini[4], N. Kucher[1], D. Spirk[5], S. Barco[1], Presenter: D. Voci[1] ([1]Zurich, [2]Padua, [3]Mainz, [4]Geneva, [5]Bern)

Objective: Peripheral artery disease (PAD) is one of the most prevalent cardiovascular diseases with more than 230 million people being affected worldwide. As highlighted by the recent guidelines of the European Society of Cardiology, data on the epidemiology of PAD is urgently needed.

Methods: We accessed the vital registration data of the Veneto region (Northern Italy, approximately five million inhabitants) covering the period 2008–2019. We computed annual age-standardized rates for PAD reported as the underlying cause of death (UCOD) or as one of multiple causes of death (MCOD). Age-adjusted odds ratios (OR) served to study the association between PAD and cardiovascular comorbidities.

Results: The age-standardized mortality rate for PAD as MCOD slightly declined from 20.4 to 18.3 in men and from 10.4 to 10.0 deaths per 100,000 population-years in women during the study period. The age-standardized PAD-related mortality rate declined from 4.7 to 4.6 in men and increased from 3.2 to 3.6 deaths per 100,000 population in women (Figure). These trends were not statistically significant. PAD contributed to 1.6% of all deaths recorded in the region. Ischemic heart disease, diabetes mellitus, and neoplasms were the most prevalent UCOD among PAD patients (Table 1). PAD was strongly associated with diabetes mellitus (OR 3.79, 95%CI 3.55–4.06) and chronic kidney diseases (OR 2.73, 95%CI 2.51–2.97) in men and with atrial fibrillation (OR 2.26, 95%CI 2.10–2.44) in women (Table 2).

Conclusion: PAD remains a substantial cause of death in the general population of this high-income region of Western Europe with marked sex-specific differences.

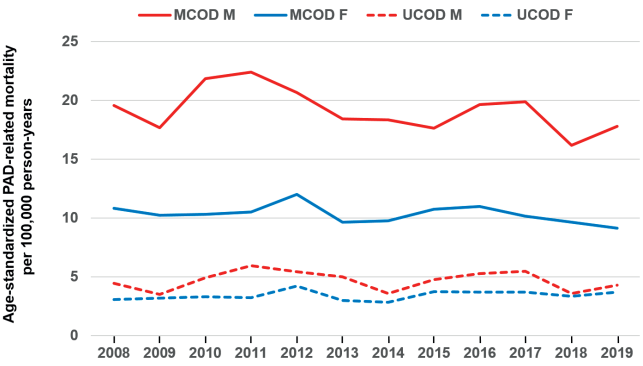

Figure. Trends in age-standardized mortality rate related to peripheral artery disease: Underlying cause and multiple causes of death. Annual age-standardized PAD-related mortality rate for multiple cause of death (MCOD) and underlying cause of death (UCOD) per 100 000 person-years in men (M) and women (F).

Table 2. Age-adjusted Odds ratios for the presence of selected conditions in the death certificates of individuals who died with peripheral artery disease, ischemic heart disease or cerebrovascular diseases (vs. none of these conditions), by gender

	OR for PAD (vs no PAD, IHD, CVD)	OR for IHD (vs no PAD, IHD, CVD)	OR for CVD (vs no PAD, IHD, CVD)
Men			
Diabetes mellitus	3.79 (95% CI 3.55; 4.06)	2.50 (95% CI 2.43; 2.56)	1.77 (95% CI 1.71; 1.83)
Atrial fibrillation	1.75 (95% CI 1.61; 1.91)	1.57 (95% CI 1.52; 1.62)	1.89 (95% CI 1.83; 1.96)
Hypertensive disease	1.52 (95% CI 1.41; 1.64)	1.84 (95% CI 1.79; 1.88)	1.78 (95% CI 1.73; 1.83)
COPD	1.26 (95% CI 1.15; 1,38)	1.30 (95% CI 1.26; 1.34)	0.83 (95% CI 0.79; 0.86)
Chronic kidney diseases	2.73 (95% CI 2.51; 2,97)	1.94 (95% CI 1.87; 2.00)	1.10 (95% CI 1.05; 1.15)
Women			
Diabetes mellitus	2.86 (95% CI 2.67; 3.07)	2.05 (95% CI 2.00; 2.11)	1.47 (95% CI 1.43; 1.51)
Atrial fibrillation	2.26 (95% CI 2.10; 2.44)	1.60 (95% CI 1.55; 1.64)	1.99 (95% CI 1.94; 2.05)
Hypertensive diseases	1.15 (95% CI 1.07; 1.23)	1.55 (95% CI 1.51; 1.58)	1.55 (95% CI 1.51; 1.58)
COPD	0.89 (95% CI 0.78; 1.01)	1.29 (95% CI 1.24; 1.34)	0.71 (95% CI 0.68; 0.75)
Chronic kidney diseases	1.94 (95% CI 1.75; 2.15)	1.66 (95% CI 1.60; 1.73)	0.91 (95% CI 0.87; 0.96)

Notes. PAD: peripheral arterial disease; IHD: Ischemic Heart Disease; CVD: Cerebrovascular disease; COPD: Chronic Obstructive Pulmonary Disease; OR: odds ratio; CI: 95% confidence interval.

Table 1. List of the selected underlying causes of death from death certificates in patients with peripheral artery disease (PAD)

Underlying cause of death	ICD-10 code	Men		Women	
		n	%	*n*	%
Peripheral artery disease	I70.2, I73.9, I74.3, I74.4	1043	23,3%	1570	33,7%
Ischemic heart diseases	I20-I25	777	17,3%	595	12,8%
Diabetes mellitus	E10-E14	635	14,2%	631	13,6%
Neoplasms	C00-D48	611	13,6%	263	5,7%
Cerebrovascular diseases	I60-I69	191	4,3%	264	5,7%
Hypertensive diseases	I10-I15	172	3,8%	279	6,0%
COPD	J40-J44, J47	117	2,6%	57	1,2%
Mental disorders	F01-F03, G30	83	1,9%	157	3,4%
Atrial fibrillation and flutter	I48	35	0,8%	98	2,1%
Total		4485		4654	

Notes. COPD: Chronic Obstructive Pulmonary Disease.

FM 2.5

Development and implementation of an ambulatory integrated care pathway tool for peripheral artery disease patients: The vascular passport – From knowledge to awareness

R. Del Giorno, S. Keller, C. Deslarzez, S. Lanzi, L. Calanca, S. Deglise, L. Mazzolai, Presenter: R. Del Giorno (Lausanne)

Objective: Despite its high prevalence, peripheral artery disease (PAD) remains an under-recognised and under- treated condition. Patients' lack of knowledge about the disease, and low awareness of its consequences contribute to this misrecognition. Additionally, none or partial implementation of existing guidelines' recommendations by physicians' results in suboptimal management of PAD patients. Integrated care pathways (ICP) represent a multi-modal approach in hospital setting to promote evidence-based treatments together with patient's empowerment in a collaborative relationship of care. We present the "Vascular Passport", an ICP developed and implemented at our angiology and vascular surgery departments. Aim of the passport is: i) to support a more standardized management of PAD patients taking into account national and international guidelines, ii) to promote patients' awareness on their disease and treatment. The final goal is to facilitate a structured and shared-decision of cardio-vascular (CV) secondary prevention for PAD patients.
Methods: Structured analysis of several current CV guidelines, in order to adapt recommendations to the local context, was firstly performed. Thereafter a local ICP model was developed.
Results: Development of an ICP vascular model based on: 1) Development of an algorithm for anti-thrombotics, and lipid-lowering therapies in secondary CV prevention; 2) Development of a patient held booklet, the "vascular passport", designed for patients and physicians to describe, record, and evaluate medical screening, treatment and results. The passport is also a tool for determining patient objectives and allow collaboration between patient, treating physician, and vascular specialists.
Conclusion: The present vascular passport is the first model of integrated care pathway, for promoting better adherence to best clinical practice in PAD and for enabling patients to understand the process and outcome of their personal care. Our long-term results on outcomes will provide the evidence of the potential wider applicability of the model in other settings.

FM 2.4

Late outcomes after fixed-dose ultrasound-assisted catheter-directed thrombolysis for acute pulmonary embolism: Single-center experience at a University Hospital

S. Zbinden, S. Barco, N. Kucher, Presenter: S. Zbinden (Zürich)

Objective: Post-pulmonary embolism (PE) impairment and chronic thromboembolism pulmonary hypertension (CTEPH) are feared complications of acute PE. It remains unknown whether ultrasound-assisted catheter- directed thrombolysis (USAT) is effective on long-term outcomes beyond its ability to reverse right ventricular dysfunction in the acute phase.
Methods: We followed patients treated with USAT, between November 2018 and January 2022, with intermediate-high- or high-risk acute PE (ESC definition). They received a standard regimen of 10 mg alteplase/catheter over 15 hours. Over long-term follow-up, we studied (i) confirmed CTEPH, (ii) post-PE persistent dyspnea, or (iii) "post-PE impairment" as defined by the combination of dyspnea with sPAP>35 mm Hg, TAPSE <1.6 cm, or RA/RV gradient >36 mmHg. We further investigated the long-term risks of death and recurrent PE over time.
Results: A total of 161 patients were treated with USAT (EKOS®, Boston Scientific, US) after a pulmonary embolism response team approach. 1 (0.6%) patient died within 30 days of PE. 35 patients could not be followed over long-term and were excluded from the analysis. Of the remaining 125 patients, a total of 49 patients (39.2%) were women, 117 (93.6%) were European, the mean age was 62.3 (SD 14.2) years and the mean BMI was 29.6 (SD 6.9). Overall, 14 (11.2%) suffered from cancer; 15 (12%) were high-risk class and 110 (88%) intermediate-high risk. 66 patients (52.8%) underwent echocardiography. The median length of follow-up was 104 (Q1; 91 – Q3; 200) days and the median length of time to echocardiography was 112 (Q1; 93 – Q3; 190) days. CTEPH was diagnosed in 2 (1.6%) patients: in one, CTEPH was pre-existing, namely present already at the time of "acute" PE, out of any reasonable doubt, whereas CTEPH was incident in the other patient. A total of 24 (19.2%) patients had persistent dyspnea and 5 (4%) had a combination of persistent dyspnea and imaging parameters. Death was recorded in 8 (6.4%) patients after a median of 591.5 (Q1; 517- Q3; 710) days: 5 of unknown etiology, 2

Table 1. Baseline characteristics

	Patients (n=125)
Demographics	
Women, n/N (%)	49/125 (39.2)
Age (years), mean (SD)	62.3 (14.2)
Race, n (% of total), European	117/125 (93.6)
BMI (kg/m2), mean ± SD	29.6 (6.9)
Comorbidities and risk factors	
Previous deep vein thrombosis, n (%)	23/125 (18.4)
Previous pulmonary embolism, n (%)	12/125 (9.6)
Cancer, n (%)	14/125 (11.2)
Surgery in the last 30 days, n (%)	5/125 (4)
Immobilization last 7 days, n (%)	17/125 (13.6)
Contraceptive, n (%)	0/125 (0)
Hormone Therapy, n (%)	1/125 (0.8)
Pregnancy, n (%)	0/125 (0)
Renal insufficiency, Glomerular filtration rate <50 ml/min, n (%)	14/125 (11.2)
Arterial hypertension, n (%)	49/125 (39.2)
Diabetes mellitus, n (%)	21/125 (16.8)
Chronic heart failure, n (%)	1/125 (0.8)
Coronary artery disease, n (%)	7/125 (5.6)
Thyroid disease, n (%)	11/125 (8.8)
Median length follow-up and echocardiography	
Time from pulmonary embolism to follow-up (days), median, (Q1, Q3)	104 (Q1; 91.3 – Q3; 200.5)
Time from pulmonary embolism to follow-up echocardiography (days), median (Q1, Q3)	112 (Q1; 92.5 – Q3; 190)

Table 2. Pulmonary embolism severity

	Patients (n=125)
Pulmonary embolism severity	
ESC high-risk class, n (%)	15/125 (12)
ESC intermediate-high risk class, n (%)	110/125 (88)
Troponin I (ng/ml), median (Q1, Q3)	64 (Q1; 38.25-Q3; 161.50)
NT- proBNP, (ng/ml), median (Q1, Q3)	1921 (Q1; 622-Q3; 4941)
RV/LV ratio by CT, mean ± SD	1.3 ± 0.2
RV/LV ratio by Echocardiography, mean ± SD	1.2 ± 0.2
Pulmonary embolism location, n (%)	Central: 117/125 (93.6) Bilateral: 121/125 (96.8)
Associated deep vein thrombosis, n (%)	89/125 (71.2)

Table 3. Outcomes

	Patients (n=125)
Co-primary outcomes	
Diagnosis of CTEPH, n (%)	2/125 (1.6)
Post-PE persistent dyspnea	24/125 (19.2)
PPEI (Post-PE persistent dyspnea + sPAP>35 mmHg, or TAPSE <1.6cm or RA/RV gradient >36 mmHg)	5/125 (4.0)
Secondary outcomes	
Death, n (%)	8/125 (6.4)
Time from pulmonary embolism to death (days)	591.5 (Q1; 517- Q3; 710)
Recurrence of pulmonary embolism, n (%)	1/125 (0.8)

related to cancer, and 1 due to pneumonia. One (0.8%) recurrent PE occurred.

Conclusion: USAT may represent an effective and safe option to improve the course of severe acute PE also in terms of long-term outcomes.

FM 2.6

Prevalent use of high-intensity statin therapy and LDL-C target attainment among patients undergoing angioplasty for peripheral artery disease: A single-center retrospective cross-sectional analysis

S. Wolf, D. Spirk, G. Forgo, T. Sebastian, D. Voci, N. Kucher, S. Barco, Presenter: G. Forgo (Zürich)

Objective: The global burden of peripheral arterial disease (PAD) is substantial. Reducing the major modifiable risk factors for non-communicable disease, including dyslipidaemia, represents a public health priority. To evaluate the prevalent adequate use of lipid-lowering therapy (LLT) and low-density lipoprotein cholesterol (LDL-C) attainment among patients with PAD of the lower extremities undergoing percutaneous transluminal angioplasty.

Methods: We screened PAD patients treated at the University Hospital Zurich (January 2012-December 2018). We excluded patients <18 years, without classifiable severity of PAD, or with missing LDL-C or medication data. In this cross-sectional study, we studied the prevalent LLT use and LDL-C values in target according to the most recent European guidelines. Available clinical data included demographic information, lipid profile, type and dose of LLT, characteristics of the artery obstruction and angioplasty.

Results: A total of 2,148 angioplasties were performed in 956 patients: 614 (64%) were men; the mean age was 70.6 (SD 11.4) years. A total of 608 (64%) had a non-critical PAD (Fontaine stage I-IIb), whereas the remaining had a critical limb ischemia or a diabetic foot syndrome. Their median LDL-C value was 2.00 (Q1-Q3: 1.50–2.60) mmol/L. In accordance to the 2016 and 2019 European Society of Cardiology guidelines, the LDL-C target of 1.8 and 1.4 mmol/L was not reached in 63% (n=599) and in 79% (n=760) of patients, respectively. Only 41% (n=390) of patients were on high-intensity statin therapy.

Conclusion: The attainment of LDL-C targets, as recommended by current European guidelines, and the use of high-intensity LLT are still unsatisfactory in the majority of PAD patients.

FM 2.3

Venous thromboembolism and its clinical sequelae in intravenous drug users: Systematic review and meta-analysis

G. Forgo, M. Szlaszynska, R.M. Fumagalli, D. Mazzaccaro, G. Nano, N. Kucher, T. Sebastian, S. Barco, Presenter: G. Forgo (Zürich)

Objective: Intravenous drug abuse continues to pose a substantial burden worldwide. Little is known on actual risk of VTE and its sequelae in this patient group.

Methods: A systematic literature search was conducted in October 2021. We included studies reporting on the prevalence of VTE and chronic venous disease (CVD) in intravenous drug users (IVDU), as well as on the prevalence of IVDU among VTE and CVD patients. Two reviewers independently selected the articles and appraised their quality. A random-effect meta-analysis was performed to pool risks across studies.

Results: We included 18 studies for a total of 7,691 patients. Overall prevalence of VTE among IVDU was 28.7% (95%CI: 19.0–39.5%). Among patients diagnosed with VTE, 14.5% (95%CI: 9.8–19.9%) were IVDU. Similar rates were confirmed with the studies published in the past decade. Reported rates of CVD ranged between 57.8% and 60.9%. The quality of evidence of the majority of the included studies was low and we could not exclude a selection bias in the studies in geographical regions with high IVDU prevalence.

Conclusion: VTE appears to be at least ten times more frequent in IVDU compared to the general population of similar age. National programs for IVDU patients should also focus on early and late VTE-associated complications. Novel endovascular approaches might improve the course of chronic vein disease and post-thrombotic syndrome in this patient population.

FM 2.1

Next-generation sequencing for the detection of somatic-mosaic mutations in extra-cranial arteriovenous malformations

S.M. Bernhard[1], Y. Döring[1,2], E. Vassella[1], U. Amstutz[1], C. Zweier[1], J. Rössler[1], L. Boon[3], M. Vikkula[3], A. Tuleja[1], G. Hamvas[1], M. Schindewolf[1], I. Baumgartner[1], Presenter: S.M. Bernhard[1] ([1]Bern, [2]Munich, [3]Brussels)

Objective: Most congenital vascular malformations (CVM) are genetically characterized by somatic mosaic pathogenic hotspot mutations, but the varying phenotypic penetration makes the association between genotype and phenotype among clinical subgroups of patients with CVM difficult. Of particular need is an understanding of genetic mutations that underlie CVM with serious medical effects and poor prospects for treatment, such as arterio-venous malformations (AVM).

Disease-targeted genetic panel testing has become a clinically useful approach in oncology for genotype targeted cancer therapy. In AVMs mosaic-activating variants in oncogenes at several levels of the RAS/MAPK signaling pathway have been described.

Methods: As part of an international interdisciplinary research project, our clinical database of the prospective Bernese VAScular COngenital Malformation (VASCOM) cohort was expanded by the implementation of standardized CVM tissue harvesting. Samples are immediately snap frozen for DNA extraction using the Qiagen® tissue kit and subsequently analyzed using high-throughput sequencing with the TruSight Oncology 500 panel (TSO500).

Results: A preliminary analysis of the TSO500 results showed 26 patients with AVM (10 males and 16 females), aged from 11 to 64 years. We detected known variants in MAP2K1 (n=6), KRAS (n=6) and RASA1 (n=1), but also not yet for extra-cranial AVM described variants related to the RAS/MAPK pathway (RIT1, PTPN11, PIK3CA, PTEN and GNAQ). No clear genotype-phenotype correlations were evident, but AVMs with KRAS variants compared to MAP2K1 variants were more frequently associated with ulcerations (67% vs 17%) and longitudinal overgrowth (83% vs 17%).

Conclusion: Our analysis of tissue biopsies from patients with congenital AVMs using TSO500, confirmed mutations as described in the literature, but also revealed that genotype-phenotype associations based on these predefined genes remain difficult. To draw definite conclusions on genotype related phenotypes the number of patients analyzed remains too small. Larger series of patients would have to be analyzed by a broadened approach with whole exome sequencing in order to get a complete picture of all involved somatic mutations.

Additionally information on expression patterns, their spatial resolution and involved cell types is needed.

FM 2.7

Characteristics and clinical course of plantar vein thrombosis: A retrospective analysis from a single center

M. Serifi, D. Voci, N. Kucher, A. Kobe, S. Barco, P.A. Kaufmann, Presenter: M. Serifi (Zürich)

Objective: The management of lower-limb deep vein thrombosis (DVT) is driven by good evidence from interventional trials and large cohort studies, as also reflected by the strength of recommendations from international guidelines. This is not the case for rare thrombosis, such as plantar vein thrombosis, for which only sparse case reports are available.

Methods: We retrospectively analyzed patients managed at the Department of Angiology of the University Hospital Zurich between 2005–2021. Patients were screened by accessing the institutional electronic database with the aid of keywords. Plantar vein thrombosis was defined as a non-compressible vein thrombosis involving any vein segment distally from the ankle, in the presence or not of symptoms. In this analysis, we aimed to describe practice-based data on clinical presentation, treatment pattern, and course of plantar vein thrombosis. The study was approved by the cantonal ethic commission and all patients provided informed consent for the use of their clinical data for research purposes.

Results: Our electronic screening resulted in a list of 45 patients for whom a "plantar vein thrombosis" (or synonyms) was mentioned in at least one medical report. After manual check of these cases, we identified 16 patients in whom the diagnosis was established. Median age was 62 (Q1-Q3: 46–73) years and 9/16 (56%) were women. All patients were symptomatic and had pain (100%) or swelling (67% of patients with available data).

The most frequent risk factors for VTE were: cancer in 6/16 (38%), chronic heart failure 2/16 (12%), prior VTE 1/16 (6%) or DVT 4/16 (25%), venous malformation 1/16 (3%), recent surgery 2/16 (12%), immobilisation 2/16 (12%). Plantar vein thrombosis was associated with distal DVT in 7 patients and with proximal DVT in one.

Thirteen patients received direct oral anticoagulants and 3 (27%) parenteral anticoagulation for a median of 90 (Q1-Q3: 90–90) days. The median overall follow-up was 17 (Q1-Q3: 5–70) months. Three recurrent events were recorded during follow-up: one pulmonary embolism, one deep vein thrombosis and one plantar vein thrombosis. No major bleeding was recorded.

Conclusion: To our knowledge, this is the first cohort study providing initial data on the characteristics and course of plantar vein thrombosis. A multicenter registry will be started with the aim of investigate rarer manifestations of VTE.

FM 3.3

New options to treat Marfan disease

S. Clerc-Rignault, C. Bielmann, K. Bouzourene, T. Déglise, C. De Nicola, L. Mazzolai, N. Rosenblatt-Velin, Presenter: N. Rosenblatt-Velin (Lausanne)

Objective: Marfan Syndrome (MFS) is an autosomal dominant inherited connective tissue disorder affecting the cardio-vascular sys-

tem. Aortic dissections and ruptures are the primary cause of morbidity and mortality in these patients. No treatment really cures Marfan patients. Interestingly, in humans, mutations in the gene coding for the C-type natriuretic peptide (CNP) or its receptors lead to a "Marfan-like syndrome". CNP is a local regulator of skeletal growth and of vascular homeostasis, remodeling and angiogenesis. CNP binds to two receptors, NPR-B and NPR-C, expressed on endothelial and smooth muscle cells (SMCs). The aim of this project is to determine whether altered CNP signaling pathway contributes to the development and progression of the vascular dysfunctions in MFS.

Methods: Plasma and vessel biopsies were taken from Marfan patients and from Fbn1C1039G/+ mice. CNP and TGF-beta concentrations were measured in the plasma. CNP, NPR-B and NPR-C protein levels were evaluated by Western blot analysis in aortic tissue during the development of MFS.

Results: Plasmatic proCNP level in Marfan patients depends on the age and the presence of thoracic aortic aneurysm (TAA). Increased levels were found in young patients presenting no or reduced TAA and decreased levels were measured in patients with TAA compared to age and sex-matched non-Marfan patients. The NT- proCNP level increased and the total TGF- and free TGF- levels decreased with age and TAA progression in Marfan patients. Immunostaining, Western blot and qRT-PCR analysis showed that CNP is decreased at the protein and mRNA levels in the aorta of Marfan patients when compared to the same aorta in non-Marfan patients. NPR-C protein level decreased in Marfan patients, whereas its mRNA level increased. TGF-beta signaling increased at the mRNA levels. In 6–7-week-old male Fbn1 +/- mice, CNP mRNA and protein levels drastically decreased in the aortic arch and ascending aorta and increased in the descending aorta. In 24-week-old Marfan male mice, CNP protein level was normalized in the different segments of the aorta. In the aortic arch and ascending aorta of female Fbn1 +/- mice, CNP mRNA and protein levels didn't change in young animals (6 weeks old) but increased in 24-week-old mice.

Conclusion: Our results suggest that a deficit in CNP could contribute to the development and progression of the disease in male mice. In contrast, in female mice, normal and higher CNP levels could protect from the progression of the MFS.

FM 3.2

Sit-to-stand muscle power is related to functional performance at baseline and after supervised exercise training in patients with lower extremity peripheral artery disease

S. Lanzi, A. Pousaz, L. Calanca, L. Mazzolai,
Presenter: S. Lanzi (Lausanne)

Objective: Patients with peripheral artery disease (PAD) have decreased muscle power contributing to functional limitations. The sit-to-stand (STS) is a validated test to assess muscle power in older individuals; however, it has never been investigated in patients with PAD. We evaluated the relationship between STS muscle power and common disease-related outcomes in patients with PAD at baseline and following supervised exercise training (SET).

Methods: This observational study investigated patients with Fontaine stage II PAD. Before and after SET, maximal treadmill walking distance (MWD), functional performance tests (six-min walk, STS, stair climbing, habitual gait speed), and quality of life (SF-36 questionnaire) were assessed. Relative (W.kg-1) STS muscle power was calculated using a validated equation. Simple and multiple regressions models were used.

Results: Ninety-five patients with PAD were included (63.1±12.1 years, 67% male). Relative STS muscle power (before: 2.7 W.kg-1 [95%CI 2.5–2.9]; after: 3.3 W.kg-1 [95%CI 3.1–3.6]), MWD (before: 367.0 m [95%IC 302.4–431.5]; after: 598.4 m [95%IC 515.6–681.3]), six-min walking distance (before: 418.3 m [95%IC 399.4–437.2]; after: 468.8 m [95%IC 452.7–484.9]), stair climbing performance (before: 6.8 s [95%IC 6.2–7.4]; after: 5.3 s [95%IC 4.9–5.7]), and habitual gait speed (before: 1.10 m.s-1 [95%IC 1.05–1.14]; after: 1.18 m.s-1 [95%IC 1.14–1.22]) significantly increased following SET (P≤.001). Similarly, physical (before: 31.4 [95%IC 29.4–33.3]; after: 35.8 [95%IC 33.9–37.7]) and mental (before: 39.5 [95%IC 37.0–42.0]; after: 43.1 [95%IC 40.9–45.4]) component summaries of the SF-36 significantly improved (P≤.001). Greater relative STS muscle power at baseline was significantly related to greater baseline treadmill (β≤.380; P≤.002) and functional (β≤.597; P≤.001) performance, and quality of life (β≤.291; P≤.050). Larger increases in relative STS muscle power following SET were associated with greater improvements in functional performance only (β≤.419; P≤.009). In contrast, there were no significant relationships between changes in relative STS muscle power and changes in treadmill performance and quality of life following SET.

Conclusion: STS test may provide a practical and easy clinical tool to monitor overall functional status before and after exercise interventions in patients with symptomatic PAD.

FM 3.5

Effects of moderate- and high-intensity exercise training in normoxia or hypoxia on atherosclerosis in mice

L. Wang[1], J. Lavier[2], K. Bouzourène[2], N. Rosenblatt-Velin[2], L. Mazzolai[2], Y. Zhang[1], G. Millet[2], M. Pellegrin[2],
Presenter: M. Pellegrin[2] ([1]Beijing, [2]Lausanne)

Objective: Moderate-intensity continuous training (MICT) is an effective strategy to reduce cardiovascular risk and atherosclerosis. High-intensity interval training (HIIT) has emerged as an alternative to MICT because of its similar or superior efficacy on cardiovascular parameters. Exercising in hypoxia may have potential clinical applications for patients with cardiovascular diseases, however the effect of hypoxic exercise, in particular the effect of hypoxic HIIT, on atherosclerosis development remains unknown. In this study, we compared the effects of MICT and HIIT in normoxia (FiO2 21%) or hypoxia (FiO2 11.2%) on atherosclerosis in adult male Apolipoprotein E Knockout (ApoE KO) mice.

Methods: Mice performed 3 sessions of exercise training per week. MICT consisted in treadmill running for 40 min at 40% of maximal running speed (MAS) while HIIT consisted in 4 sets of 5 x 10-s sprints treadmill running at 100% of MAS with 20 s of rest between sprints and 5 min between sets.

Prevention study: ApoE KO mice were fed a high-fat diet (HFD) for 6 weeks. At the start of HFD, mice were randomly allocated into six groups: sedentary in normoxia (SED-N), sedentary in hypoxia (SED-H), MICT in normoxia (MICT-N), MICT in hypoxia (MICT-H), HIIT in normoxia (HIIT-N), and HIIT in hypoxia (HIIT-H).

Therapeutic study: ApoE KO mice were fed HFD for a total of 18 weeks and were randomly allocated during the last 6 weeks to the same 6 groups than in the prevention study. Histological sections of the aortic sinus were processed for quantification of total atherosclerotic plaque area.

Results: Prevention study: Atherosclerotic plaque area was significantly reduced both in MICT-N and HIIT-N compared to SED-N ($p<0.001$). SED-H mice exhibited smaller plaque area than SED-N ($p<0.05$). No significant differences were observed between MICT-H and MICT-N, as well as between HIIT-H and HIIT-N. Plaque area did not significantly differ between the three hypoxic groups. Therapeutic study: No significant differences were found between the six groups.

Conclusion: MICT and HIIT, independently of normoxic or hypoxic conditions, were equally effective at preventing the development of atherosclerotic plaques in ApoE KO mice. Hypoxia did not potentiate the beneficial preventive effect of exercise training on atherosclerosis. However, passive hypoxic exposure was efficient in preventing atherosclerotic plaques development in sedentary mice.

FM 3.4

Popliteal artery aneurysm: Preliminary results of a population screening

S. Ruttkowski, S. Deglise, L. Mazzolai, A. Alatri,
Presenter: S. Ruttkowski (Lausanne)

Objective: Popliteal artery aneurysm (PAA) is frequently asymptomatic but, as abdominal aortic aneurysm (AAA), has potentially dramatic consequences resulting in arterial thrombosis and/or peripheral embolism with higher risk of limb ischemia and permanent sequalae (mainly amputation). Data about prevalence and natural history of PAA are very limited in men and absent in women.

Moreover, the benefit of PAA screening has never been assessed so far. We aim to evaluate, by a population screening, the prevalence and characteristics of PAA.

Methods: Monocentric, observational, prospective, Swiss cohort study. The following were included: men aged ≥65 years; women ≥65 years with history of smoking or arterial hypertension; men or women aged ≥55 years with familial history of aneurysm. Subjects with known or previously operated aneurysm as well as patients received aneurysmal screening in the last 12 months were excluded.

Results: At the time of our analysis, 252 consecutive subjects, 53% men and 47% women, were screened. Median age was 69.2 and 70.4 years in men and women, respectively. We found 3 (2.3%) PAA in men and none in women. All three patients had a history of smoking. None of the patients required vascular surgery in the following 12 months. Concerning cardiovascular risk factors distribution, 70.7% of men was former or current smokers (vs 66.4% in women, $p= 0.564$). No differences in body mass index, dyslipidemia, and arterial hypertension were found in the two groups. Conversely, chronic renal failure and diabetes were more frequent in men.

Conclusion: The preliminary results of our study showed a non-negligible prevalence of PAA in men and highlighted the importance of PAA screening, considering the potential dramatic consequences of disease. These data need to be confirmed in a large sample-size. A multicentric international study, based on an opportunistic screening for PAA, is currently ongoing (NCT05360108).

FM 3.1

Non-dissecting distal aortic and peripheral arterial aneurysms in patients with Marfan syndrome

Q. Pellenc[1,2], A. Boitet[2], Y. Castier[2], O. Milleron[2], G. Jondeau[2],
Presenter: Q. Pellenc[1,2] ([1]Morges, [2]Paris)

Objective: In Marfan syndrome (MFS), aortic or peripheral arterial dilatation is usually the consequence of aortic dissection. Non-dissecting distal aortic and peripheral aneurysms (DAPA) are barely described. We sought to determine the incidence and prognostic impact of non-dissecting DAPA requiring surgical repair in a large population of patients with MFS.

Methods: Patients referred to the French MFS Referral Center were included in a prospective database, and patients treated for a non-dissecting DAPA between 2013 and 2020 were retrospectively reviewed. First line therapy was open surgery. Patients unfit for open repair or experiencing life-threatening complication underwent endovascular repair.

Results: Among 1575 patients with MFS, 19 (1.2%) were operated for 25 non-dissecting DAPA. The mean age was 42.4±11.5 years. Non-dissecting DAPA involved the subclavian or axillar artery (n=12), the descending or thoracoabdominal aorta (n=6), the abdominal aorta and iliac arteries (n=6), and the popliteal artery (n=1). Open and endovascular repairs were performed in 22 and 3 cases, respectively. After a median follow-up of 54.2 months, no local recurrence was noticed and no secondary procedure was performed. Eight patients presented a new aortic event including 2 aortic dissections and 7 new aortic surgeries. Compared to the overall MFS population, the non-dissecting DAPA group presented a significantly higher risk of aortic event (100% vs 28%, $p<0.0001$), a higher risk of aortic dissection (53% vs 8%, $p<0.0001$) (Figure), and a higher rate of pejorative genetic mutations (68% vs 40%, $p=0.011$).

Conclusion: Among patients with MFS, the diagnosis of non-dissecting DAPA requiring surgery is infrequent but associated with a significantly adverse outcome, thus advocating for a specific follow-up.

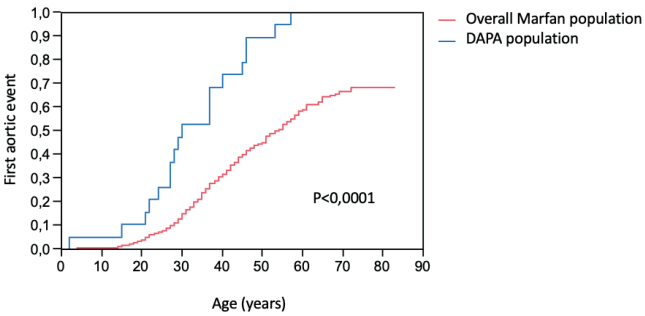

Figure. Kaplan-Meier estimation of first aortic events (Ascending and distal aortic Aneurysm surgery or Aortic dissection) occurrence in DAPA (Distal aortic and peripheral aneurysm) population and in the overall population of Marfan syndrome patients with FBN-1 mutation.

P 6

A new tool for improving cardiovascular risk prediction: The FHRAB score

R. Del Giorno, M. Reveilhac, L. Mazzolai, M. Depairon, R. Darioli, Presenter: R. Del Giorno (Lausanne)

Objective: Subclinical atherosclerosis detection at carotid and femoral sites by the atherosclerosis burden score (ABS) improves cardiovascular (CV) risk stratification beyond traditional CV risk factors. Objectives. To explore if combining the ABS score with the FHRS, the FHRAB Score, enhances CV risk prediction.
Methods: Prospective observational cohort study of 1024 patients without previous CV disease. ABS score, i.e. sum of number of carotid and femoral plaques, was assessed at baseline examination. Yearly follow-up for incident major adverse cardiac events (cardiovascular death, myocardial infarction, stroke and peripheral arterial revascularisation) was carried out. Receiver operating characteristic curve (ROC-AUC) of FHRS, ABS, and FHRAB Score, were compared.
Results: 60 primary CV events (5.8%) observed over a median follow-up of 6.0±3.3 years. The ROC-AUC for CV events prediction increased from 0.676 for FHRS alone to 0.744 after ABS addition ($p < 0.001$). FHRABS showed the highest CV predictive performance (Youden Index 43% vs 31% for FHRS alone).
Conclusion: FHRAB Score improves CV prediction of the FHRS. FHRABS represents an easy -to-use, radiation- free tool to improve the detection of patients at high CV risk and to promote a more personalized CV prevention in clinical practice. Further studies are advocated to validate a wide implementation of the FHRABS score in daily clinical practice.

P 9

Arterial tortuosity in patients with rare vascular diseases

X. Luta, M. Fresa, G. Buso, M. Kirsch, S. Deglise, J. Bouchardy, F. Zanchi, L. Mazzolai, Presenter: X. Luta (Lausanne)

Objective: Increased arterial tortuosity index (ATI) has been associated with various cardiovascular and respiratory complications. However, the extent and relevance to rare vascular diseases remain to be fully elucidated. We describe ATI in patients with rare vascular diseases and the association with clinical and demographic characteristics.
Methods: This is a retrospective analysis of patients included in the RAVAD registry who were followed at the Malformation and Rare Vascular Disease Center, Lausanne University Hospital (Switzerland).

Computed tomography (CT) images of patients were retrieved between January 2019 and April 2022. Patients with rare vascular disease were compared to patients with suspected rare vascular diseases, and inflammatory arterial diseases. ATI was measured as the ratio of aortic length to geometric length. Multivariate logistic regression was used to determine the association of ATI and potentially relevant predictors of arterial tortuosity including age, gender, diagnosis, and lesion type.
Results: One hundred eighty-two patients were included in the study. The mean age upon CT scan was 46.2 years, 67.6% of patients were aged ≥ 40, and 61.5% were females. ATI was more pronounced in patients with arterial dissection and aneurysm (mean, 1.09 [SD, 0.26]; N=59) compared to those with fibromuscular dysplasia (mean, 1.02 [SD, 0.17]; N=30), inflammatory arterial diseases (mean, 0.97 [SD, 0.19]; N=43) and connective tissue diseases (mean, 0,97 [SD, 0.20], N= 37). Our analysis demonstrated that ATI was higher in patients aged ≥ 40 compared to those aged < 40 (1.1 vs. 0.86; $p < 0.05$) and was significantly correlated with height, hypertension, and presence of arterial ectasia/aneurisms ($p < 0.05$).
Conclusion: Our preliminary results suggest that ATI increases with age, height, hypertension and the presence of ectasia/aneurism. Although further studies are needed, measurement of ATI may be of value in evaluating prognosis of vascular conditions in patients with rare vascular diseases.

Gefässchirurgie

FM 1.2

Amputation-free survival after distal crural or pedal bypass surgery for chronic limb threatening ischemia

C. Kohler, K. Gaizauskaite, V. Makaloski, J. Schmidli, S. Weiss, Presenter: C. Kohler (Bern)

Objective: Chronic limb threatening ischemia (CLTI) is associated with a relevant risk of limb loss and death. The aim of this study is to analyze amputation-free survival, WIfI (Wound, Ischemia and Foot Infection) and GLASS (Global Limb Anatomic Staging System) classification in patients who underwent distal crural or pedal bypass, defined by a distal anastomosis in the distal third of the crural arteries or the foot.
Methods: Single-centre retrospective case series. We analyzed all patients who underwent distal crural and pedal bypass for CLTI from 2010 – 2019. Follow-up data was collected until December 2020.
Results: Thirty-two distal crural and pedal bypasses in thirty-one patients suffering from CLTI were performed. Median age was 67 years (range 21–86), 81% were male and 48% had diabetes. Ninety-four percent of limbs were preoperatively staged as GLASS III and 53% were classified WIfI stage 4. Fourteen patients (44%) had undergone failed endovascular revascularization. Bypass material was the great saphenous vein (GSV) in 22, arm vein in 6, polytretrafluorethylen in 3, and a composite of Omniflow II and GSV in 1 patient. Thirty-day mortality was 19% (n=6, none with major amputation). Median follow-up for the remaining patients was 59 months (range 17 – 128 months). Thirty-day major amputation rate was 12% (n=4). Estimated major amputation-free survival at 1, 2, 3, 4 and 5 years was 80%, 74%, 58%, 51% and 32%. Seven of all eleven major amputations during follow-up were initially WIfI stage 4.
Conclusion: In patients who require distal crural or pedal bypass for CLTI, amputation-free survival during the first two years is acceptable, but the risk of limb loss or death is high thereafter. The WIfI classification may help to identify those patients who will benefit from distal crural or pedal bypass surgery.

FM 1.1

Percutaneous thrombectomy with the JETi6 device for the treatment of acute renal artery thrombosis with renal failure

A. Cottier, R. Emsley, L. Arts, C. Haller, Presenter: A. Cottier (Sion)

Objective: Renal artery thrombosis (RAT) is a rare disease which causes decreased renal blood flow and can result in permanent renal damage and subsequent arterial hypertension. Cardiac embolization is the most frequent cause, however in situ thrombosis of an underlying atherosclerotic stenosis is not uncommon.
Methods: Acute renal failure was seen in a 79-year-old woman following acute thrombosis of the renal artery. Percutaneous thrombectomy of the right renal artery was performed with the JETi6 device under local anaesthesia as well as complementary stenting for underlying atherosclerotic renal artery stenosis.
Results: Complete recanalization of the right renal artery was obtained using the JETi6 device and complementary stenting. Postoperative ultrasound showed adequate renal perfusion. The patient s renal function and blood pressure was rapidly normalized. Follow-up at 1 month showed no complications.
Conclusion: Endovascular thrombectomy allows rapid flow restoration, with more efficient preservation of renal function and fewer hemorrhagic complications, compared to thrombolysis alone. This is a unique report highlighting the efficacy and safety of the JETi6 thrombectomy device in the treatment of acute in situ renal artery thrombosis.

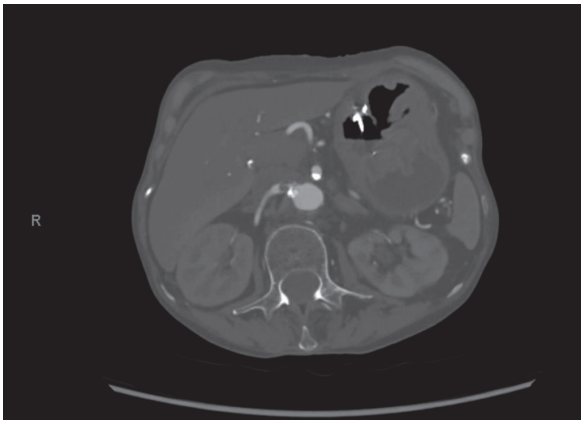

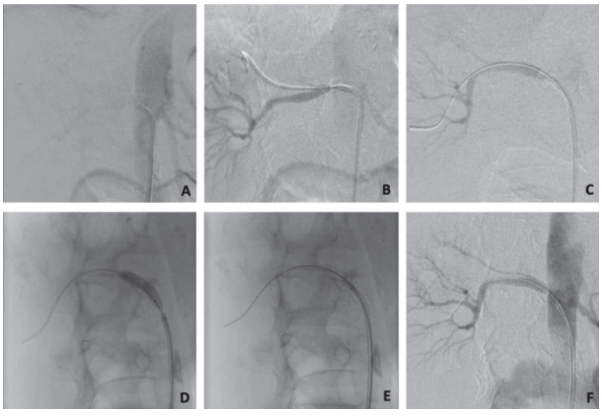

Figure.

FM 1.4

Vessel preparation with chocolate PTA ballon catheter in femoropopliteal lesions

L. Zimmermann, H. Probst, P. Fillet, Q. Pellenc, S. Vedani, F. Saucy, Presenter: L. Zimmermann (Morges)

Objective: Vessel preparation before angioplasty with a drug-coated balloon (DCB) in femoropopliteal lesions is crucial to improving drug delivery efficacy to the arterial wall. Plain old balloon angioplasty is still used to prepare the vessel, but limitations such as dissection and residual stenosis are frequently observed. This study aims to evaluate the efficacy and safety of a nitinol-caged balloon (Chocolate PTA balloon Catheter) associated with DCB in femoropopliteal lesions.
Methods: This observational retrospective study was conducted on all consecutive patients receiving nitinol caged balloon angioplasty for femoropopliteal lesions from 2020 to 2021. Vessel preparation was performed using the Chocolate PTA balloon, followed by systematic drug-eluting balloon inflation. The duplex scan and clinical visit guaranteed the follow-up. The patency rate and clinical-driven target revascularisation (CDTLR) were analysed using Kaplan Meier. Standard statistical analysis was used to evaluate the safety and efficacy of the treatment.
Results: 35 patients (18 males; the median age of 77 years) were included suffering from intermittent claudication (58.3%) or chronic limb-threatening ischemia (38.9%). The Global Limb Anatomic Staging System (GLASS) for the 35 limbs analysed included 2 (5.7%) stage1, 18 (51.4%) stage 2 and 15 (42.9%) stage 3. The median length of the lesions was 67 48.1 mm. Occlusion of the superficial femoral artery was present in 12.5%. All patients were treated with a nitinol-caged balloon followed by DCB (93.8%), and the bailout stenting rate was 28.6% (10/35), mainly related to type C dissection. Major adverse events and unplanned major amputation occurred in 2.9% of the cases. The mean follow-up was 8.6 at 4.7 months; the primary patency was 96.8% at six months.

Freedom from CDTLR was 96.8% at six months. ABI at six months was significantly higher concerning preoperative values (p=0.035).
Conclusion: These early results demonstrated that combining a Chocolate PTA balloon catheter and a drug-eluting balloon is safe and efficient even if the bailout stenting rate is still too high, which is also related to the early experience with this device.

FM 1.3

Outcome of endovascular aortic repair in hostile neck anatomies before and after launching GORE® EXCLUDER® conformable endoprosthesis

S. Hofer, M. Furrer, Presenter: S. Hofer (Chur)

Objective: The conformable GORE Excluder stentgraft system (CXT) for severe kinked necks up to 90 degree has become available in Europe since March 2019. The aim of this study was to compare the outcome after EVAR in hostile necks before and after launching CXT.
Methods: Between April 2015 and March 2022 160 EVAR were performed at our institution. 80 patients with AAA were treated before and 80 after the introduction of CXT in our centre. Hostile neck was

defined as severe kinking (>60°) or conic neck. The outcome of these patients was analyzed retrospectively regarding endoleak type IA (EL IA), sack growth and neck related reintervention rate.
Results: Before and after launching CXT we identified 36 (45%) (Gr1) and 37 patients (46%) (Gr2) with hostile neck anatomies. In Gr1 the aneurysms were excluded by endoprosthesis with suprarenal fixation (n=12) or by GORE EXCLUDER endoprosthesis (n=24). In Gr2 the patients were treated by CXT (n=34) otr other stentgraft systems (n=3). The median follow-up time in Gr1 was 39, in Gr2 7 months. EL IA appeared in GR1 in 16 patients and in Gr2 in 12 patients, two of them were not treated by CXT. EL IA resolved sponteneously during follow up in 7 patients in Gr1 versus 9 of Gr2. In Gr1 reintervention rate was 12 patients out of 36 (33%) (OR 6.406, 95% CI 1.64–25.01) versus 3 out of 37(8%) in Gr2. None of the CXT patients needed reintervention and all showed sac shrinking during follow-up.
Conclusion: CXT is a promising stentgraft system in hostile neck anatomy. The reintervention rate can be lowered by using this conformable stentgraft. Primary EL IA often seems to resolve spontaneously and sac shrinkage can be observed. An important limitation of this study is the short follow-up time in Gr2.

YI 5

Predictors and consequences of sac shrinkage after endovascular infrarenal aortic aneurysm repair

S. Vedani[1], S. Petitprez[1], E. Weinz[1], J.-M. Corpataux[1], S. Déglise[1], C. Deslarzes-Dubuis[1], E. Côté[1], J.-B. Ricco[2], F. Saucy[3], Presenter: S. Vedani[1] ([1]Lausanne, [2]Poitiers, [3]Morges)

Objective: Aneurysm shrinkage has been proposed as a marker of successful endovascular aneurysm repair (EVAR). We evaluated the impact of sac shrinkage on secondary interventions, survival and its association with endoleaks and compliance with instructions for use (IFU).
Methods: This observational retrospective study was conducted on all consecutive patients receiving EVAR for an infrarenal abdominal aortic aneurysm (AAA) using exclusively Endurant II/IIs endograft from 2014 to 2018. Sixty patients were entered in the study. Aneurysm sac shrinkage was defined as decreased ≥5 mm of the maximum aortic diameter. Univariate methods and Kaplan-Meier plots assessed the potential impact of shrinkage.
Results: 26 patients (43.3%) experienced shrinkage at one year, and 34 (56.7%) had no shrinkage. Shrinkage was not significantly associated with any demographics and morbidity except hypertension (p = .01). No aneurysm characteristics were associated with shrinkage.

Non-compliance with instructions for use (IFU) in 13 patients (21.6%) was not associated with shrinkage. Three years after EVAR, freedom from secondary intervention was 85±2% for the entire series, 92.3±5.0% for the shrinkage group and 83.3±9% for the no-shrinkage group (Logrank: p=.49). Survival at three years was not significantly different between the two groups (85.9±7.0% vs 79.0±9.0%, Logrank; p=.59). Strict compliance with IFU was associated with less reinterventions at three-year (92.1±5.9% vs 73.8±15%, Logrank: p=.03).

Similarly, survival at three years did not significantly differ between strict compliance to IFU and non compliance (81.8±7.0% vs 78.6±13.0%, Logrank; p=.32).
Conclusion: This study suggests that shrinkage ≥5 mm at 1-year is not significantly associated with a better survival or a lower risk of secondary intervention than no-shrinkage. In this series, the risk of secondary intervention regardless of shrinkage seems to be linked more to non-compliance with IFU. Considering the small number of patients, these results must be confirmed by extensive prospective studies.

YI 3

Open surgical repair of a large renal artery aneurysm: Technical note

C. Schürmann, M. Menth, H.-L. Chan, E. Psathas (Fribourg)

Objective: Renal artery aneurysms are rare lesions that are almost universally diagnosed incidentally. They can be extra- or intra-parenchymal and etiologically related with arteritis, fibromuscular dysplasia, renal artery dissection or primary aneurysmal degeneration. Rapidly expanding lesions or those greater than 30 mm should be considered for repair, in order to prevent rupture and kidney loss.
Methods: A 54-year-old male patient was referred to our department due to the incidental finding of a 35 mm asymptomatic aneurysm of the distal left renal artery upon abdominal CT-angiography (Figure 1). Preoperative glomerular filtration rate (GFR) was normal and nuclear renal scan showed symmetric kidney participation. Due to the localization and the multiple distal renal branches arising from the aneurysm sac, endovascular repair was considered unsuitable and the patient was scheduled for open repair. Under general anesthesia, exposure of the distal part of the left renal artery was performed through a median laparotomy and right median visceral rotation anteriorly to the Gerota fascia. Further mobilization of left renal vein caudally, allowed for the proximal and distal control of all the main arteries arising from the aneurysm (Figure 2). After systemic anticoagulation, the proximal and distal branches of the renal artery were clamped, and a longitudinal incision was performed at the cephalad part of the aneurysm sac. The orifices of all three outflow branches were identified and the most cephalad part of the aneurysmal sac was excised (Figure 3). Aneurysmorraphy with direct suturing of the remaining sac was performed, with a total renal ischemic time of 12 minutes (Figure 4). After de- clamping, a normal Doppler waveform was obtained on each individual outflow artery. Further banding of the remaining sac was performed using an 8mm PTFE graft.
Results: The postoperative period was uneventful, with intact renal function and the patient returned home after 10 days. Follow-up imaging with CT-angiography and nuclear renal scan at 1 month, revealed patency of all three outflow renal arteries, with no residual arterial stenosis or renal ischemia. (Figure 5). Repeat follow-up imaging at one year was planned.

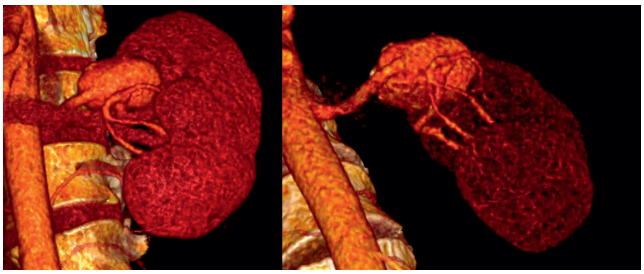

Figure 1. CTA 3D reconstruction showing the aneurysm of the distal left renal artery measuring 35mm in diameter.

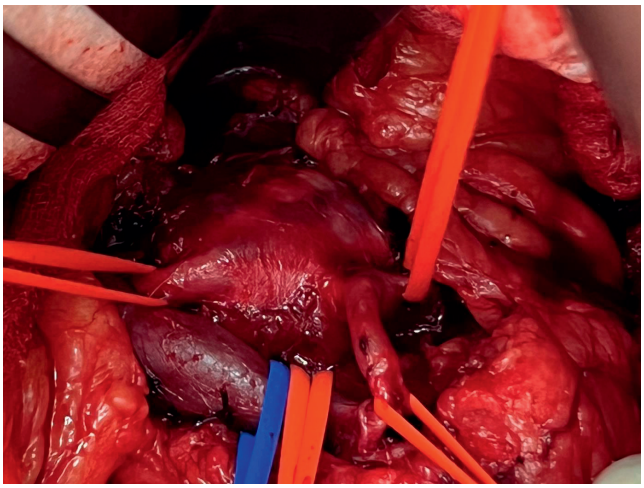

Figure 2. Intraoperative image showing the multiple distal renal branches arising from the aneurysm sac and controlled with vessel loops (red) and the caudally retracted left renal vein (blue).

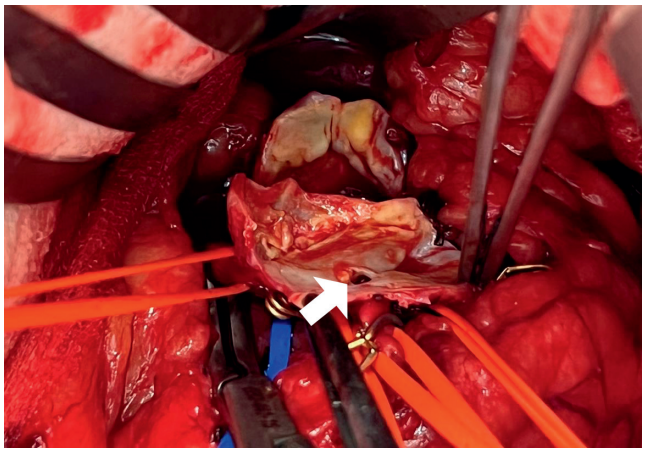

Figure 3. Intraoperative image showing the clamped proximal and distal branches of the renal artery and the longitudinal incision at the cephalad part of the aneurysm sac. The orifices of the outflow branches are identified (arrow).

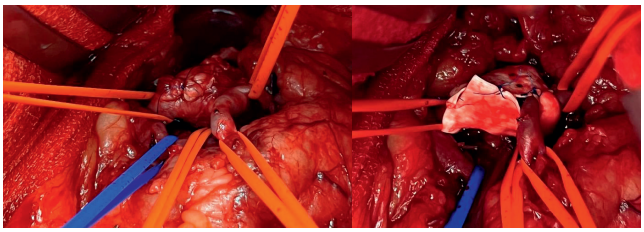

Figure 4. Intraoperative image showing the direct suture of the remaining sac (left) and banding with an 8 mm PTFE graft (right).

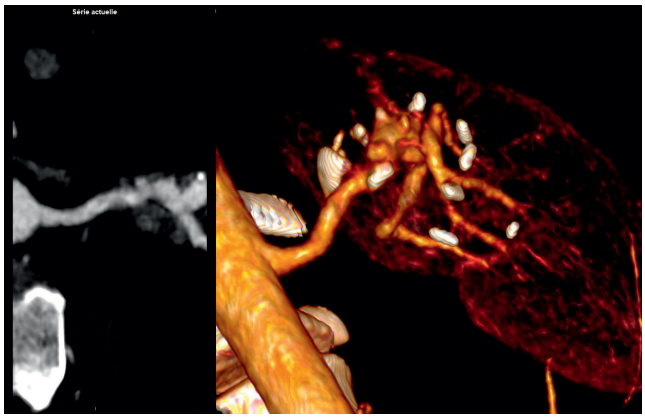

Figure 5. Postoperative CTA showing the reduction of the aneurysm sac, and patency of all major outflow arteries.

Conclusion: When multiple distal branches arise from the aneurysm sac, open repair remains the best option in fit patients. Operative techniques vary from ex-vivo reconstruction, venous bypass, resection with direct anastomosis, patch angioplasty to aneurysmorraphy with banding. Surgeons should be prepared to adapt their strategy based on the anatomy and perioperative local findings. Aneurysmorraphy allows for minimal renal ischemia and preservation of multiple outflow vessels, however long-term follow- up is recommended to exclude further aneurysmal degeneration of the remaining aneurysmal sac.

P 10

Recurrent perigraft seroma after carotid-subclavian bypass surgery: A case report

E. Lonfat, M. Kostrzewa, P. Buntschu, S. Engelberger,
Presenter: E. Lonfat (Baden)

Objective: Symptomatic subclavian artery stenosis is nowadays preferably treated by endovascular means. When endovascular treatment is not successful however, carotid-subclavian bypass or transposition may be offered. Either Dacron or ePTFE grafts may lead to possible local complications like perigraft seroma.
Methods: After failure of endovascular recanalization of a symptomatic left subclavian stenosis, a 75-year-old female underwent a carotid-subclavian bypass with a silver-coated Dacron graft. Seven months later the patient presented with an ischemic left hand as well as subclavian swelling and tenderness. Bypass occlusion as well as a seroma were detected on Duplex ultrasound. The subclavian occlusion was then successfully recanalized and stented by an endovascular approach from the groin and the arm simultaneously. The seroma relapsed even after several puncture attempts. The successive samplings showed no bacterial growth. Due to the symptoms caused by compression, the graft was surgically removed. The common carotid artery needed segmental reconstruction by a Dacron interposition graft due to severe intimal hyperplasia and scarring at the anastomotic site.

Two months later the patient presented with swelling and redness in the jugular fossa. A fluid collection with connection to the common carotid vascular reconstruction was diagnosed on CT scan. Surgical revision with drainage of the collection and reconstruction of the common carotid artery with autologous vein were then performed. The microbiological workup including sonication of the graft material did not show any contamination.
Conclusion: Perigraft seroma may occur in up to 4% of cases of vascular reconstructions, regardless of the type of graftmaterial used. Significant morbidity can thus occur. Dacron and ePTFE are though preferred in carotid- subclavian reconstructions over the use of autologous veins. Carotid-subclavian transposition remains an alternative without implication of graft material.

P 7

Concomitant aortic and celiac artery compression by right diaphragmatic crus: A rare cause of abdominal and lower limb claudication

L. Zimmermann, F. Saucy, H. Probst,
Presenter: L. Zimmermann (Morges)

Objective: Symptomatic compression of the celiac trunk is a rare condition mainly associated with aortic constriction. The present report describes a case of aortic and celiac artery compression by right diaphragmatic crus presenting as severe epigastric pain and lower limb claudication.
Results: A 41-year-old woman with an unremarkable medical history presented with epigastric pain after meal intake and sports activity without weight loss. Prolonged physical activity was also associated with claudication of the lower limbs. Computed tomography (CT) scan of the abdomen revealed compression of the aorta and the celiac artery by a left hypertrophic diaphragmatic crus. A dynamic CT scan was also made and confirmed the compression at inspiration. After an adequate preoperative assessment, we performed laparoscopic decompression by section of the right diaphragmatic crus on the anterior part of the aorta, just above the celiac artery. No complication occurred. The patient was discharged home three days after and declared a complete resolution of the epigastric pain and claudication.
Conclusion: A hypertrophic diaphragmatic crus may compress concomitantly aorta and celiac trunk associated with specific symptoms. Dynamic CT is essential for diagnosis and laparoscopic section its treatment.

P 8

Ruptured popliteal aneurysm: Experience in a secondary care hospital

E. Lonfat, P. Buntschu, U. Schneider, C. Kalka, M. Birrer,
S. Engelberger, Presenter: E. Lonfat (Baden)

Objective: Popliteal aneurysm accounts for 70% of all peripheral arterial aneurysms. Nonetheless, it is a rare entity with an incidence of 0.1%. Besides thrombosis and embolization, rupture accounts for 2.2% of the complications. Open repair is still considered the gold standard, due to limited data on the results of endovascular repair. In our secondary care hospital, two patients benefit from open vascular repair after the rupture of a popliteal aneurysm.
Results: A 83-year-old patient presented with acute pain and swelling of the right leg. A CT scan revealed a popliteal aneurysm (10 cm), invalidating the primary diagnosis of venous thrombosis. The arterial reconstruction was performed with an autologous venous interposition graft. Due to impossible tension-free closure of the fascia and to prevent a compartment syndrome, a fasciotomy of the medial thigh and the anterolateral compartment of the leg was performed. The postoperative follow-up was uneventful with good patency of the graft at 5 months. An 88-years-old patient presented with

Figure 1. CT-scan of case 1.

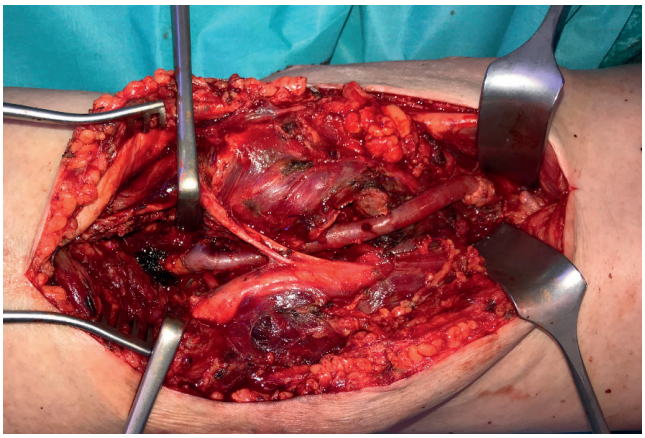

Figure 2. Reconstruction of the popliteal artery with autologous vein.

chronic right leg pain for three weeks. A CT scan showed a ruptured aneurysm (12 cm), as well as a non-ruptured aneurysm (4.5 cm) of the popliteal artery. Due to the long defect, the vascular repair was performed with an Omniflow II graft. In the absence of signs of compartment syndrome, a fasciotomy was not needed. Postoperatively, nervous lesions of the sciatic, peroneal and tibial nerves persisted probably due to the long compression effect of the aneurysm on the neural structures. The patient died 3 months later from hospital-acquired pneumonia.

Conclusion: Popliteal aneurysm rupture, although relatively rare, is encountered in secondary care hospitals.

Prompt surgical intervention is essential for limb salvage. Open surgical repair provides good long-term patency despite possible postoperative complications. Urgent endovascular repair may be the treatment of choice for frail patients, despite possible higher adverse events.

Figure 3. CT-scan of case 2.

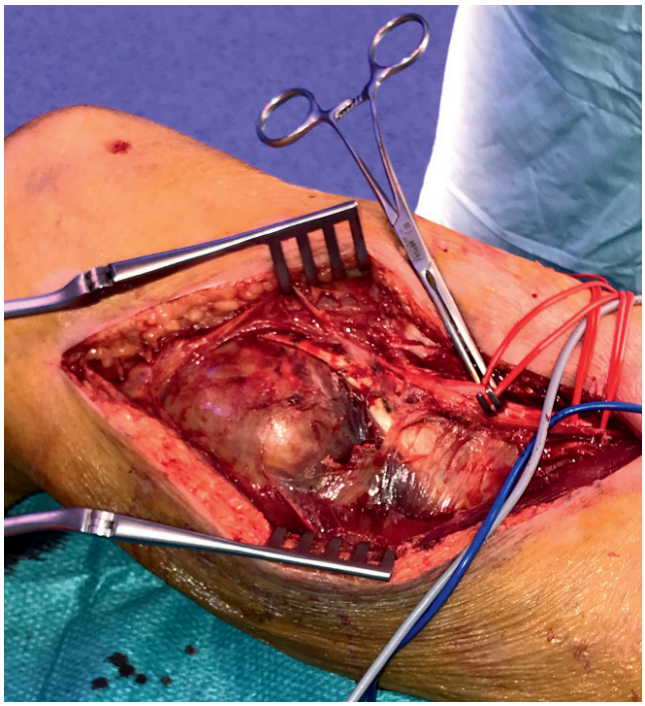

Figure 4. Intraoperative exposure of popliteal aneurysm.

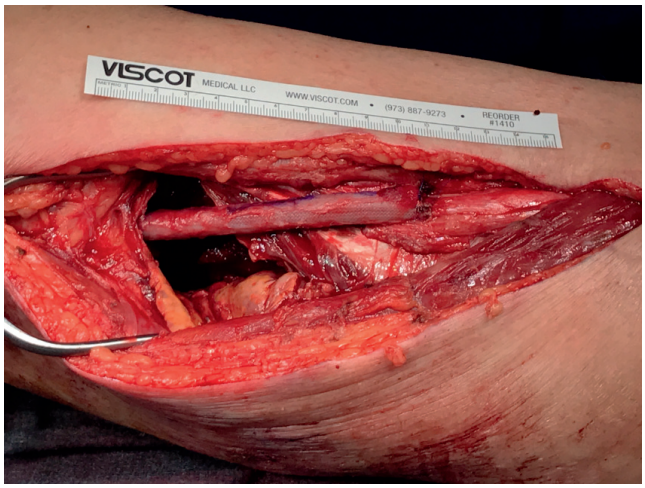

Figure 5. Reconstruction of the popliteal artery with Omniflow II graft.

Phlebologie

FM 2.2

Prevention in phlebology: From utopia to reality

J. Ragg, S. Kreis, Presenter: J. Ragg (Zürich)

Background: In everyday phlebology practice there is an abundance of products and recommendations that claim to be important for the prevention of venous diseases. However, evidence-based data on primary and secondary prevention are very scarce. Which preventive measures can currently be considered sufficiently justified and practicable?
Methods: Together with the Prevention Working Group of the DGP (Deutsche Gesellschaft für Phlebologie) and by help of international experts presenting during the annual meetings in 2020–2022, 434 relevant original works and 55 guidelines were viewed with the aim of an updated re-evaluation of potential preventive measures.
Results: An excellent data situation was found for anticoagulant therapy, with the exception of the prevention of thrombosis in Covid-19 infection, which has only been relevant since 2020. The use of medical compression stockings appears to reliably reduce edema and improve symptoms, but no proof exists for the prevention of CVI or varicose veins. Similarly, there is only weak evidence for so-called venotonics, and causal evidence of effectiveness is largely lacking. The greatest scientific deficit was found for the prevention of primary venous insufficiency, as early stages are still completely undifferentiated or even absent in common classifications.
Conclusion: While in the past a lot of professional attention has been devoted to the prophylaxis of acute and serious phlebological diseases such as thrombosis and venous embolism, this is not the case for the socio-economically highly relevant "chronic" disease of primary venous insufficiency. There is a considerable need to catch up here for research, medical training, and professional policy evaluation.

SSMVR

SFC 1.1

ADAMTS18+ villus tip telocytes maintain a polarized VEGFA signaling domain and fenestrations in nutrient-absorbing intestinal blood vessels

J. Bernier-Latmani[1], C. Mauri[1], R. Marcone[1], F. Renevey[1], S. Durot[2], L. He[3], M. Vanlandewijck[3,4], C. Maclachlan[1], S. Davanture[1], N. Zamboni[2], G. Knott[1], S. Luther[1], C. Betsholtz[3,4], M. Delorenzi[1], C. Brisken[1], T. Petrova[1], Presenter: J. Bernier-Latmani[1] ([1]Lausanne, [2]Zurich, [3]Uppsala, [4]Huddinge)

Objective: The small intestinal villus tip is the first point of contact for lumen-derived substances including nutrients and microbial products. Electron microscopy studies from the early 1970s uncovered unusual spatial organization of small intestinal villus tip blood vessels: their exterior, epithelial-facing side is fenestrated, while the side facing the villus stroma is non-fenestrated, covered by pericytes and harbors endothelial nuclei. Such organization optimizes the absorption process, however the molecular mechanisms maintaining this highly specialized structure remain unclear.
Methods: We analyzed intestinal villus tips in multiple mouse models by 3D whole-mount immunostaining and serial-block face scanning electron microscopy. Furthermore, mechanistic insights were drawn from single cell RNAseq data of small intestinal fibroblasts. We also analyzed portal and tail vein metabolites.
Results: We report that perivascular LGR5+ villus tip telocytes (VTTs) are necessary for maintenance of villus tip endothelial cell polarization and fenestration by sequestering VEGFA signaling.

Mechanistically, unique VTT expression of the protease ADAMTS18 is necessary for VEGFA signaling sequestration through limiting fibronectin accumulation.
Conclusion: We propose a model in which LGR5+ ADAMTS18+ telocytes are necessary to maintain a "just-right" level and location of VEGFA signaling in intestinal villus blood vasculature to ensure on one hand the presence of sufficient endothelial fenestrae, while avoiding excessive leakiness of the vessels and destabilization of villus tip epithelial structures.

SFC 1.2

Characterization of physiological and pathological angiogenesis at the single cell level

G. Turiel[1], T. Gorski[2], J. Zhang[1], T. Desgeorges[1], N. Tisch[1], Presenter: G. Turiel[1] ([1]Zurich, [2]Zürich)

Objective: Angiogenesis is a highly regulated mechanism of new blood vessels formation. This process has been extensively characterized during development and in some pathological conditions through the tip-stalk cell model. However, whether angiogenesis is similar or not during physiological and pathological conditions is still not fully understood. In fact, the role for other angiogenic mecha-

nisms, such as intussusception, is not clearly identified. Therefore, the aim of this project is to characterize, at the cellular and molecular level, whether angiogenesis is a conserved response or it adapts depending on the physiological or pathological condition.

Methods: We have applied 3 different mouse models to study angiogenesis in skeletal muscle. Exercise as a model for physiological angiogenesis as well as cardiotoxin injection and hindlimb ischemia as models for pathological angiogenesis. We have identified in each intervention the angiogenic peak through FACS analysis of endothelial cell (EC) proliferation. Subsequently, we have performed single cell RNA sequencing for each individual model at the angiogenic peak to characterize and compare the cellular and molecular angiogenic response in each condition.

Results: Pathological angiogenesis showed a faster angiogenic response compared to the physiological condition. In both pathological models the angiogenic peak was identified 3 days after each intervention whereas the physiological model showed a slower and milder response with the angiogenic peak after 7 days of exercise. Interestingly, when we analysed each model using single cell RNA sequencing, all models showed the appearance of 2 new EC populations responsible of the angiogenic response. Different analysis at the single cell level as well as subsequent experiments targeting these 2 populations showed an important role and interaction of these populations in the angiogenic response.

Conclusion: We have identified a similar angiogenic response at the cellular and molecular level in different pathological and physiological conditions. Although the angiogenic response could originate from different causes, we identified the appearance of the same 2 EC populations in every condition that seem to coordinate angiogenesis in a similar way. Therefore, these results suggest that angiogenesis could harbour a conserved mechanism independent of the pathological or physiological scenario.

SFC 1.3

Brain endothelial antigen presentation detains CD8+ T cells at the blood-brain barrier leading to its breakdown

S. Aydin[1], J. Pareja[1], N. Page[2], E. Kaba[1], U. Deutsch[1], A. Johnson[3], M. Schenk[1], D. Merkler[2], B. Engelhardt[1], Presenter: J. Pareja[1] ([1]Bern, [2]Geneva, [3]Rochester, MN)

Objective: Multiple sclerosis (MS) is a chronic neuroinflammatory demyelinating disease targeting the central nervous system (CNS). Blood-brain barrier (BBB) breakdown and increased immune cell trafficking into the CNS are early pathological hallmarks of MS. CD8 T cells are an abundant immune cell subset infiltrating the CNS in MS patients but the mechanisms regulating their entry into the CNS remain incompletely understood. Antigen presentation at the BBB was proposed to promote CD8 T-cell entry into the CNS. Here, we aim to understand the role of antigen- (cross) presentation by the BBB endothelial cells to CD8 T cells, and its role in neuroinflammation.

Methods: To study the antigen presentation on the brain endothelial cells under inflammation, we make use of primary mouse brain microvascular endothelial cell cultures stimulated with TNF alpha and INF gamma, which are co-cultured with naive and effector OT-I CD8 T cells. In order to study this phenomenon in vivo, we use the ODC-OVA mice, which express ovalbumin as a Neo-self antigen in the CNS, to induce a CD8 T cell mediated neuroinflammation. Two-photon intravital microscopy is then used to image the dynamics of OT-I CD8 T cells at the BBB in vivo.

Results: Here we demonstrate that BBB endothelial cells are able to uptake protein antigens and effectively present them in an MHC class I restricted manner to CD8 T cells in vitro. Brain endothelial antigen presentation suffices to prime naïve CD8 T cells in vitro driving their proliferation and differentiation into short-lived effector cytotoxic CD8 T cells, which eventually leads to brain endothelial cell apoptosis. Additionally, under physiological flow brain endothelial antigen- presentation reduced general post-arrest CD8 T cell mobility, decreasing their speed and displacement, as well as CD8 T-cell crawling and diapedesis rates. In a CD8 T cell driven neuroinflammation mouse model, both naïve and effector CD8 T cells arrested more efficiently on the BBB under neuroinflammation, where antigen-dependent interactions also lead a reduced crawling speed and displacement of the effector CD8 T cells over the BBB endothelium.

Conclusion: Taken together our data suggest that brain endothelial antigen cross-presentation prohibits CD8 T cell entry into the CNS and rather triggers CD8 T-cell mediated focal BBB breakdown and thus exacerbates neuroinflammation.

SFC 1.4

Lateral induction of Dll4 expression initiates intussusceptive angiogenesis by VEGF and its inhibition promotes therapeutic angiogenesis in muscle

R. Gianni Barrera[1], A. Uccelli[1], M. Trani[1], R. Blanco[2], K. Bentley[3], H. Gerhardt[4], A. Banfi[1], Presenter: R. Gianni Barrera[1] ([1]Basel, [2]London, [3]Boston, [4]Berlin)

Objective: VEGF can induce either normal or aberrant angiogenesis depending on its dose in the microenvironment around each producing cell in vivo. Recently we have shown that VEGF over-expression in skeletal muscle induces microvascular growth by an initial circumferential enlargement followed by intussusception. Here we investigated how the Dll4/Notch1 pathway regulates vascular enlargement and splitting by VEGF rather than sprouting.

Methods: Monoclonal populations of transduced myoblasts, expressing specific VEGF levels that induce normal or aberrant angiogenesis, were implanted in mouse muscles.

Results: By 4 days the circumferentially enlarged vessels induced by VEGF displayed simultaneous Notch1 activation and Dll4 expression in long stretches of adjacent endothelial cells. Within 14 days post cell implantation, when intussusceptive remodeling was complete, the Dll4/Notch1 axis was no longer active in either normal or aberrant vascular structures. Early Notch inhibition disrupted the enlargements into disorderly endothelial aggregates. Testable scenarios were generated by a computational model for the dynamics of Dll4 expression and NICD activation as a function of VEGF dose. Experimental validation of these predictions provided evidence that VEGF leads tocontiguous expression of Dll4 and Notch1 activation in adjacent endothelial cells by a mechanism of lateral induction of Dll4 by activated Notch1. Remarkably, Notch inhibition during therapeutic VEGF delivery in skeletal muscle was therapeutically beneficial, as normal angiogenesis by moderate VEGF levels was further stimulated and newly induced micro-vascular networks were functional and phys-

iologically perfused. These results are opposite to those reported in conditions of sprouting angiogenesis, where Notch blockade caused instead dysfunctional vascular growth and worsened perfusion.

Conclusion: These data suggest that Notch signalling regulates intussusceptive angiogenesis in an opposite fashion to sprouting, through a mechanism of lateral induction of Dll4 expression by activated Notch1. These results bear translational relevance, since therapeutic angiogenesis by VEGF delivery to skeletal muscle takes place through the mechanism of intussusception and not sprouting. In fact, Notch inhibition leads to opposite outcomes compared to conditions of sprouting angiogenesis, increasing both vascular growth and functional perfusion.

SFC 2.1

Subarachnoid erythrocytes clear to cervical lymphatic vessels and can recirculate in the systemic circulation

A. Madarasz, S. T. Proulx, Presenter: A. Madarasz (Bern)

Objective: Subarachnoid hemorrhage (SAH) comprises 5% of all strokes but is associated with a mortality of up to 50%. Proposed processes by which red blood cells (RBCs) leave the subarachnoid space (SAS) intact or in degraded form are: erythrolysis, erythrophagocytosis and efflux along cerebrospinal fluid (CSF) drainage routes. Studies in mice have shown that outflow of CSF is mainly along perineural structures of cranial and spinal nerves, with the efflux pathways from the cranial nerves leading to superficial (scLN) and deep cervical lymph nodes (dcLN). Our aim is to elucidate the mechanisms of RBC clearance from the SAS, as a deeper understanding could lead to new therapeutic approaches to mitigate brain injury.

Methods: We perform autologous blood injections into the cisterna magna in Prox1-EGFP reporter mice for lymphatics. Blood drawn from the saphenous vein is labeled with the lipophilic far-red dye DiD and mixed with pegylated P40D800 near-infrared (NIR) dye; a total of 3µl is injected. In vivo NIR stereomicroscopy of the blood vessels of the ear is performed to detect labeled RBCs in the systemic circulation. Possible drainage pathways for RBCs to extracranial lymphatics are evaluated in vivo and postmortem.

Results: Labeled cells are circulating within the systemic vasculature 30 min. after injection. The dcLNs and lymphatic collectors contain labeled cells after 15 min. In scLNs labeled cells are visible after 25–30 min.

Simultaneously, they appear in the collecting lymphatics draining from the orbit. The same lymphatics were also draining tracer from the SAS. Postmortem in-situ imaging and histology show perineural accumulations of cells, especially around the optic and olfactory nerves and DiD label in the lymphatics of the nasal cavity.

Conclusion: To our knowledge these results are the first to show that RBCs can rapidly leave from the subarachnoid space via lymphatics and recirculate in the systemic circulation. The similar dynamics between tracer and cells regarding their efflux to the cervical lymphatics from the cribriform plate and the eye imply open pathways that do not impose a barrier for cells. Whilst discontinuation in the arachnoid layer at the exit points of the olfactory nerves from the olfactory bulb has been observed, the optic nerve seems to have a sheet of arachnoid up until the entry into the eye bulb, implying the need for further investigation in this area.

SFC 2.2

Role of the angiogenic factor Angiopoietin-2 in monocyte-derived macrophage recruitment into the healthy and inflamed central nervous system

K. Berve[1], C. Schwab[1], S. Barcos[1], U. Deutsch[1], G. Locatelli[1,2], B. Engelhardt[1], Presenter: K. Berve[1] ([1]Bern, [2]Basel)

Objective: In multiple sclerosis (MS) infiltrating monocyte-derived macrophages are the predominant inflammatory cells within central nervous system (CNS) lesions and significantly contribute to disease severity and outcome. Studies in MS patients and its animal model experimental autoimmune encephalomyelitis (EAE) have shown elevated levels of the endothelial angiogenic factor angiopoietin-2 (Ang-2) in the blood and CNS while antibody mediated blocking of Ang-2 was shown to ameliorate EAE. The present study therefore aims to specifically decipher the role of endothelial Ang-2 in monocyte-derived macrophage migration across the blood- brain-barrier (BBB) into the CNS in neuroinflammation.

Methods: We have established a transgenic mouse model with endothelial cell-specific and inducible overexpression of human Ang-2 crossed into the CX3CR1+/GFP/CCR2+/RFP myeloid cell reporter mouse. This allows us to distinguish the role of endothelial overexpressed Ang-2 on GFP+ CNS-resident myeloid cells versus CNS infiltrating RFP+ monocyte-derived macrophages during steady state and EAE.

Results: We observed that endothelial overexpression of Ang-2 increased the number of CCR2+ macrophages but also of CD3+ T-lymphocytes in the brain of male but not of female mice at steady state.

Immunofluorescence analysis of CNS cryosections revealed that those immune cell infiltrates were however confined to the laminin+ leptomeningeal compartment while the CNS parenchyma was devoid of CCR2+ macrophages and CD3+ T-cells. Studying EAE development with endothelial Ang-2 overexpression led to the surprising observation that male but not female transgenic mice presented with an ameliorated disease course.

Conclusion: Our present data suggests sex-specific effects of endothelial Ang-2 in neuroinflammation potentially mediated by differential regulation of myeloid cell recruitment to the CNS.

SFC 2.3

Characterization of Xpr1 heterozygous mice as an animal model for primary familial brain calcification

U. Maheshwari[1], R. Ni[2], S. Bertazzo[3], F. Szeri[4], M. Greter[1], A. Keller[1], Presenter: U. Maheshwari[1] ([1]Zürich, [2]Zurich, [3]London, [4]Budapest)

Objective: Mutations in XPR1, Xenotropic and Polytropic Retrovirus Receptor 1, gene are known to cause primary familial brain calcification (PFBC) in humans. It is an autosomal inherited neurodegenerative disease characterized by the presence of abnormal vascular calcifications in the basal ganglia.

Clinical phenotypes associated with PFBC are variable ranging from asymptomatic patients to highly affected patients presenting

neuropsychiatric disorders. So far, four causative genes, namely PDGFB, PDGFRB, XPR1, and SLC20A2 have been identified to cause autosomal dominant-PFBC (AD-PFBC) in humans.

However, the pathomechanisms underlying formation of brain vascular calcification in PFBC patients remain poorly understood. This study aims to understand the role of XPR1, the only known inorganic phosphate exporter in metazoans, in development and progression of brain vessel associated calcifications in mice.

Methods: We utilized a combination of histological stainings, immunohistochemistry, fluorescent confocal microscopy, light-sheet microscopy, electron microscopy (EM), magnetic-resonance imaging (MRI), and blood plasma electrolyte analyses to characterize brain vessel associated calcifications and their progression in Xpr1 heterozygous mice. We also investigated the changes in cellular components of neurovascular unit surrounding vascular calcifications in these mice.

Results: Here, we report that brain vascular calcification in Xpr1 het mice are localized to thalamus and first observed in 7 month old animals and the calcification phenotype worsens with age. We also observed a sexual dimorphic worsening of calcification phenotype with larger nodules appearing in aged males. We identified widespread occurrence of reactive astrocytes and microglia in deepbrain region suggesting a change in brain homeostatic state. We also observed expression of osteogenic markers around calcified nodules.

Conclusion: We have characterized a new mouse model for PFBC where vessel associated calcifications are observed in heterozygous animals, a phenotype previously observed only in homozygous mouse models of AD- PFBC related genes (PDGFB hypomorphs [Pdgfbret/ret] and Slc20a2 loss of function [Slc20a2-/-]). Our data provides a closer insight into progression of PFBC in humans and role of phosphate balance in maintaining a homeostatic state in brain vasculature.

SFC 2.4

Rapid self-assembly of stable and functional microvascular networks in vitro and in vivo by VEGF- decorated fibrin matrices

A. Rouchon[1], P.S. Briquez[2], D.J. Schaefer[1], J.A. Hubbell[2], N. Di Maggio[1], A. Banfi[1], Presenter: A. Banfi[1] ([1]Basel, [2]Chicago)

Objective: Generation of functional vascular networks is an unresolved challenge for 3D engineered tissues, both in vitro to produce vascularized organoids and in vivo to promote progenitor survival and differentiation. Signaling by the angiogenic master regulator VEGF is physiologically regulated by interaction with the extracellular matrix. Here we decorated fibrin hydrogels with an engineered VEGF protein to generate an optimal matrix-associated angiogenic microenvironment.

Methods: Fibrin matrices contained 10 mg/ml human fibrinogen, 3U/ml thrombin, 3U/ml factor XIIIa, endothelial cells (HUVEC) and adipose stromal cells (ASC) as support perivascular cells. VEGF164 protein was fused to the transglutaminase substrate peptide NQEQVSPL (TG-VEGF) to enable its covalent cross-linking to fibrin.

Results: HUVEC+ASC co-culture rapidly self-assembled into physiologically differentiated vascular networks, with physiological apico-basal polarization and patent lumens. Optimal vessel formation was achieved with 10 mg/ml fibrinogen, containing 5x10E6 cells/ml with 100 ng/ml of TG-VEGF, yielding a 2.5-fold improvement vs no-VEGF controls after both 7 and 14 days. TG-VEGF significantly accelerated endothelial proliferation speed, as shown by pospho-histoneH3. Vessel diameters remained compatible with micro-circulation (median=17 µm). Human-derived vascular structures formed after 7 days of in vitro culture could rapidly connect to the host vasculature upon subcutaneous implantation and were efficiently perfused by the systemic circulation. TG-VEGF both accelerated the formation and perfusion of hybrid vessels and improved graft invasion by the host vessels. Notably, human-derived vascular networks rapidly regressed in vivo in the absence of TG-VEGF.

Conclusion: Fibrin decoration with 100 ng/ml of TG-VEGF promotes the efficient self-assembly of 3D, perfusable, lumenized and physiologically differentiated micro-vascular networks within 7 days. Upon implantation in vivo, TG-VEGF specifically enabled rapid connection to the host vessels within 3 to 7 days to support blood perfusion and was required for the microvascular network persistence and continued function. This engineered angiogenic microenvironment can be exploited both for the generation of in vitro vascularized organoids and for the rapid in vivo vascularization of 3D tissue engineered grafts.

P 11

Endothelial transmembrane adaptor protein MYCT1 limits nutrient uptake and consumption by the white adipose tissue endothelium

L. Wetterwald, A. Köck, S. Arroz-Madeira, B. Prat-Luri, M. Delorenzi, A. Sabine, T. Petrova, Presenter: A. Köck (Lausanne)

Objective: The endothelium is a critical interface between the blood circulation and the tissue environments, satisfying the tissues demands for oxygen and nutrients. The highly vascularized white adipose tissue (WAT) is the body's storage depot for excess energy, leading to obesity upon excessive nutrient intake. Endothelial cells are active regulators of tissue homeostasis and endothelial dysfunction has emerged as a hallmark of metabolic disease.

Results: Here we identify the endothelial transmembrane adaptor protein Myct1 as a regulator of adult WAT expansion. Mice with endothelial-specific Myct1 ablation display lower body weight and decreased WAT, even under high-fat diet. We used a combination of in vitro and in vivo approaches to decipher underlying molecular mechanisms and found that Myct1 is necessary to limit endothelial endocytosis and an amino acid-dependent hyperactivation of mTOR signaling.

Conclusion: These results advance our understanding of how endothelial cells sustain tissue homeostasis through a complex regulation of nutrient uptake, consumption and transfer to the parenchyma.

P 12

Mechanosensitive mTORC1 signaling maintains lymphatic valves

A. Sabine, C. Saygili-Demir, M. Gong, O. Dormond, T.V. Petrova, Presenter: A. Sabine (Lausanne)

Objective: Homeostatic maintenance and repair of lymphatic vessels are essential for health. We investigated the dynamics and the molecular mechanisms of lymphatic endothelial cell (LEC) renewal in adult mesenteric quiescent lymphatic vasculature.
Methods: We used label-retention, lineage tracing and cell ablation strategies.
Results: 1) Unlike during the development, adult LEC turnover and proliferation was confined to the valve regions of collecting vessels, with valve cells displaying the shortest lifespan. 2) Proliferating valve sinus LECs were the main source for maintenance and repair of lymphatic valves. 3) We identified mechanistic target of rapamycin (mTOR) complex 1 (mTORC1) as a mechanoresponsive pathway activated by fluid shear stress in LECs. Depending on the shear stress level, mTORC1 activity drives division of valve cells or dictates their mechanic resilience through increased protein synthesis. 4) Overactivation of lymphatic mTORC1 in vivo promoted supernumerary valve formation.
Conclusion: Our work provides insights into the molecular mechanisms of maintenance of healthy lymphatic vascular system.

P 13

Stapled 10Panx1 analogs as a new class of anti-inflammatory Panx1 channel inhibitors

M. Tournier[1], A. Lamouroux[2], V. Bes[1], F. Molica[1], M. Vinken[2], S. Ballet[2], B.R. Kwak[1], Presenter: M. Tournier[1] ([1]Geneva, [2]Brussels)

Objective: Pannexin1 (Panx1) channels allow the passage of ions and small metabolites (e.g. ATP) between the cytosol and extracellular environment. Disproportionate opening of Panx1 channels has been related to a plethora of inflammatory diseases in which ATP signaling plays a key role, like cardiac ischemia/reperfusion (I/R) injury. The goal of our study is to develop a stable Panx1 channel blocker using a known peptide-based inhibitor 10Panx1 as reference.
Methods: Combinations of global and local constraints were introduced within the peptide backbone and in vitro channel inhibition was measured by ATP release and Yo-Pro-1 uptake assays in B16-BL6 cells subjected to a hypo-osmotic shock (HOS) to increase Panx1 channel opening.
Results: Macrocyclization of the peptide backbone at different positions did no longer inhibit ATP release for most of the 10Panx1 analogs. Only two of the cyclic compounds (i.e., SBL-PX1-42 and SBL-PX1-44) were able to reduce HOS-induced ATP release by 38.8% and 33.3%, respectively (100uM, N=3–4, p<=0.05). Noteworthy, Panx1 channel inhibition was bidirectional; SBL-PX1-42 and SBL-PX1-44 also inhibited Yo-Pro-1 uptake by 25.6% and 27.2% (N=3, 100uM, p<=0.01) with a tendency for better efficacy than 10Panx1. Dose-response ATP release assays demonstrated an optimal Panx1 channel inhibition at 12.5uM. To further improve SBL-PX1-42 and SBL-PX1-44, the staple/linker length, orientation and stereochemistry were chemically modulated leading to modest improvements of the inhibitory capacity. Importantly, the in vitro stability of SBL-PX1-42 was increased by >=30-fold in human plasma compared to 10Panx1 (66.1+/-0.5 min vs. 2.3+/-0.1 min). Thereafter, the inhibitory capacities of the 10Panx1 stapled analogs were determined in endothelial cells (ECs), a cell type that is highly implicated in cardiac I/R injury. SBL-PX1-42 and SBL-PX1-44 were also able to inhibit both ATP release and Yo-Pro-1 uptake in ECs. The specificity of these two lead peptidomimetics was tested in H9c2 cells, a cardiomyocyte-like cell line that does not express Panx1. As expected, HOS did only induce a modest ATP release in these cells, which was not affected by the compounds.
Conclusion: SBL-PX1-42 and SBL-PX1-44 are promising Panx1 channel blocking compounds and further peptide modifications will lead to an optimal peptidomimetic for the in vivo use to treat cardiovascular inflammation.

P 14

Pannexin1 regulates lymphatic endothelial function

A. Ehrlich, Presenter: A. Ehrlich (Geneva)

Objective: The lymphatic system is a network of capillaries and collecting lymphatic vessels allowing for the unidirectional transport of interstitial fluids to the blood circulation. Lymphatic vessels are crucial for tissue fluid homeostasis, absorption of dietary fats and trafficking of dendritic cells (DCs) to draining lymph nodes (dLNs). Panx1 channels are formed by oligomerization of seven Panx1 proteins and allow for the diffusion of ions and signaling molecules between the cytosol and the extracellular space. We recently observed impaired lymphatic function in a Panx1-deficient mouse model for atherosclerosis (Panx1-/-Apoe-/-). However, the exact role of Panx1 in lymphatic function remains unknown.
Methods: Panx1 expression in lymphatics was assessed by immunofluorescence confocal microscopy. Using mice with inducible deletion of Panx1 in lymphatic endothelial cells (LECs), i.e. Prox1-CreERT-2Panx1fl/fl; hereafter called Panx1LECdel, and Panx1fl/fl control mice, we studied lymphatic drainage after footpad injections with Evans blue and we measured tail swelling with a caliper. Dietary fat absorption was investigated with an oral lipid tolerance test. We performed skin contact hypersensitivity assays to investigate DC migration.
Results: Panx1 was observed in LECs of lymphatic capillaries, lacteals and lymph nodes. We found decreased lymphatic drainage (25%, P<0.05; N=12) in Panx1LECdel mice compared with Panx1fl/fl controls.

Panx1LECdel mice also exhibited tail swelling (P<0.05; N=12), indicating edema formation upon Panx1 deletion from LECs. Dietary fat absorption was also impaired in Panx1LECdel mice as evidenced by decreased triglycerides and free fatty acids levels (P<0.05; N=9) compared with Panx1fl/fl mice 2 hours after oral administration of olive oil. The percentage of migratory DCs arriving in draining LNs was comparable in Panx1LECdel and control mice, suggesting that Panx1 is dispensable for regulatory DC–LEC interactions.
Conclusion: In conclusion, Panx1 in LECs displays an essential role in the maintenance of tissue fluid homeostasis and dietary fat absorption by regulating lymphatic transport efficiency.

P 15

Endothelial glut1 controls muscle insulin sensitivity through angiocrine osteopontin- mediated activation of resident muscle macrophage

J. Zhang[1], K.A. Sjøberg[2], F.Q. Li[1], T. Desgeorges[1], S. Durot[1], R. Ardicoglu[1], E. Masschelein[1], E.D. Abel[3], S. Kon[4], A. Klip[5], N. Zamboni[1], M. Kopf[1], E.A. Richter[2], K. De Bock[1], Presenter: J. Zhang[1] ([1]Zurich, [2]Denmark, [3]Iowa, [4]Fukuyama, [5]Toronto)

Objective: We explored the role of endothelium in muscle glucose transport and maintenance of muscle glucose homeostasis.
Methods: We generated endothelial-specific glut1 knock-out mice and subject the mice to hyperinsulinemic-euglycemic clamp studies to evaluate the glucose uptake in peripheral tissue. To explore the mechanism that involved in the development of insulin resistance in skeletal muscle after endothelial glut1 deletion. We charactered macrophage subpopulations by using flow cytometric method. To investigate the macrophage contribution to the development of insulin resistance in skeletal muscle after endothelial glut1 deletion. We removed the macrophages in skeletal muscle via anti-csf1r or anti-OPN antibody treatment.
Results: We found that loss of endothelial glucose transporter 1 (glut1) did not affect transendothelial glucose transport into muscle, but reduced muscle glucose uptake via inducing muscle insulin resistance. Endothelial glut1 deletion increased angiocrine osteopontin (OPN/SPP1) secretion, which promoted the proliferation and expansion of resident muscle macrophages that acted as cellular amplifiers of OPN secretion. Consequently, inhibiting resident muscle macrophage proliferation using an anti-CSF1R antibody or upon anti-OPN treatment prevented macrophage accumulation, reduced OPN levels and improved muscle insulin sensitivity in endothelial glut1 deletion mice. Mechanistically, the increase in OPN upon deletion of Glut1 was ceramide-dependent and promoting ceramide accumulation using palmitic acid increased OPN release. Finally, high-fat diet feeding reduced Glut1 expression, increased OPN levels and resident macrophage proliferation.
Conclusion: Our data illustrate how the endothelium creates a niche that controls resident muscle macrophage phenotype and function and directly links resident muscle macrophages to the development of muscle insulin resistance.

P 16

Analysis of the role of the BBB junctions in the extravasation of melanoma cells across the blood brain barrier as a crucial step in brain metastasis formation

A. Wegmüller, F. Saltarin, U. Deutsch, B. Engelhardt, R. Lyck, Presenter: A. Wegmüller (Bern)

Objective: A serious complication during melanoma is the formation of brain metastases. To successfully colonize the brain, metastatic melanoma cells must extravasate across the tight blood-brain barrier (BBB). Extravasation involves shear-resistant arrest of the melanoma cells to the BBB, followed by melanoma cell intercalation. Our research focusses on the mechanisms of these two steps to provide insights for event-tailored drug development to inhibit melanoma brain metastasis. The aim of this study is to investigate the role of BBB cell-cell junctions in melanoma cell intercalation.
Methods: In vitro live cell imaging was used to monitor the intercalation of melanoma cells into the BBB. For behavioral analysis, melanoma cell arrest on the BBB was performed under flow conditions. Freshly isolated primary mouse brain microvascular endothelial cells (pMBMECs) from LifeAct-GFP transgenic or VE-cadherin- GFP knock-in mice served as a fluorescently labeled tight in vitro model of the BBB to analyze total number of melanoma cell intercalation events (LifeAct-GFP) or the pathway of melanoma cell intercalation (VE-cadherin- GFP). To study the effect of compromised junctions of the BBB, pMBMECs were isolated from LifeAct- GFP+/PECAM-1-knockout (-ko) mice.

The degradation of PECAM-1 by the intercalating melanoma cells was studied by time-limited co-cultures of melanoma cells seeded on mouse brain derived immortalized endothelioma cells (bEnd.5), followed by protein isolation, SDS-PAGE and Western blotting.
Results: After arrest, intercalation of melanoma cells into the in vitro BBB occurs within 30 to 90 minutes. The intercalation takes place exclusively into the cell junctions of the in vitro BBB. During junctional intercalation, disappearance of the VE-cadherin-GFP signal precedes melanoma cell spread.

Consistently, endothelial junctional PECAM-1 is degraded within 60 minutes in co-cultures with melanoma cells. Finally, a direct comparison of PECAM-1-ko with PECAM-1-wild-type (wt) LifeAct-GFP pMBMECs showed that melanoma cell intercalation is significantly increased when the BBB junctions are impaired.
Conclusion: Compromised cell-cell junctions of the BBB facilitate intercalation of melanoma cells and thus extravasation. We conclude that any treatment that compromises BBB integrity should be considered as an additional risk factor for melanoma brain metastases.

P 17

Sodium Thiosulfate, a hydrogen sulfide donor, reduces inflammation but impairs vascular remodeling and promotes abdominal aortic aneurysm expansion

C. Bechelli, D. Macabrey, S. Urfer, M. Lambelet, S. Déglise, F. Allagnat, Presenter: C. Bechelli (Lausanne)

Objective: Abdominal aortic aneurysm (AAA) is a disease of the aortic wall that affects 5% of the 65 years old plus population. AAA is usually asymptomatic and 80% of rupture are fatal. Therefore, we need to find new therapeutic approaches to slow down AAA progression. Hydrogen sulfide (H2S) is an endogenous gazotransmiter produced through the reverse transulfuration pathway. In the vascular system, the main enzyme responsible for H2S production is the cystathionine-g-lyase (CSE). H2S is well known for his anti-inflammatory and anti-oxidants proprieties in the vascular system. The aim of the study was to investigate the effects of sodium thiosulfate (STS), a H2S donor, on AAA progression in WT and LDLR-/- mice.
Methods: Experiments were performed on 10 weeks old male WT or hypercholesterolemic LDLR-/-, as well as CSE-/- mice on a C57BL/6J genetic background. AAA was induced by applying topical elastase

on the abdominal aorta for 10 minutes. Sodium thiosulfate (STS) was supplemented in drinking water at 4g/L, with or without 0.2% Beta-aminopropionitrile (BAPN) for 2 weeks post-AAA. All aortas were harvested 2 weeks post- AAA. Inflammation in the aortic wall was evaluated with immunohistochemistry (IHC) staining of CD86, CD3, CD206, and MPO. Vascular remodeling was evaluated using calponin, SMA IHC and Herovici staining.

Results: STS increased the AAA size in WT and LDLR-/- mice with or without BAPN treatment. Preliminary data suggest that STS impaired vascular remodeling mice, leading to formation of larger AAA. In contrast, STS seemed to decrease inflammation in the aortic wall, especially macrophages M1 infiltration. Consistent with our data, CSE-/- mice with reduce H2S production developed smaller AAA than WT mice.

Conclusion: In conclusion, STS has a dual effect on AAA progression. On the one hand, it decreases inflammation in the aortic wall. On the other hand, it impairs vascular remodeling, leading to larger AAA. Further experiments will be performed using shorter or lower STS concentration to leverage the anti-inflammatory properties of STS while maintaining vascular remodeling.

P 18

Altered endothelial tight junction protein expression in ruptured human intracranial aneurysms

A.F. Cayron, S. Morel, P. Bijlenga, E. Allémann, B.R. Kwak, Presenter: A.F. Cayron (Geneva)

Objective: Intracranial aneurysms (IAs) are abnormal enlargements in cerebral arteries. IA rupture induces subarachnoid hemorrhage which in 1/3 of cases results in severe disability or death. The decision to treat an unruptured IA by microsurgery is based on clinical scores, and is supported by magnetic resonance imaging (MRI) showing vessel wall enhancement (VWE) in the IA wall. VWE reflects a local accumulation of colloid contrast agent and is considered a marker of IA wall instability. The pathophysiology of VWE is unknown but enhanced permeability of arterial endothelium has been proposed as a potential mechanism. The objective of our study is to investigate the expression of endothelial tight junction (TJ) proteins in human IA domes in the context of IA wall instability. To this end, we have compared human ruptured and unruptured IA domes from a Swiss IA biobank.

Methods: Human IA domes from the middle cerebral artery were obtained after microsurgery, formol fixed, embedded in paraffin, sectioned and stained for the endothelial cell marker protein CD31, the junctional proteins Claudin-5, Zonula occludens-1 (ZO-1), VE-Cadherin and Connexin43 (Cx43). Results are expressed as median (interquartile range), and compared using the Mann-Whitney U test.

Results: Endothelial cell coverage tended to be decreased in ruptured IAs (N=16) in comparison to unruptured IAs (N=30) (27% [10–49] vs. 38% [23–77], P=0.06). Interestingly, the immunosignals of TJ proteins Claudin-5 (1.70um [1.52–2.04]) and ZO-1 (2.29um [1.96–2.75]) were lower in ruptured than in unruptured IAs (Claudin-5: 2.15um [1.90–2.76], P<=0.05; ZO-1: 2.66um [2.40–3.66], P<=0.05). The signals of adherens junction protein VE- cadherin and gap junction protein Cx43 were not different in ruptured and unruptured IAs (Cx43: 1.78um [1.60–1.94] vs. 1.56um [1.30–1.83]; VE-cadherin: 2.66um [2.32–3.57] vs. 2.76um [2.37–3.53]).

Conclusion: The endothelium in ruptured human IAs has a lower expression of Claudin-5 and ZO-1 than the endothelium in unruptured IAs. No differences were observed for Cx43 and VE-cadherin. We hypothesize that reduction in TJ proteins may lead to an increased endothelial permeability favoring accumulation of MRI contrast agent in the IA wall, and thus lead to the observation of VWE. Changes in endothelial characteristics and permeability may represent a new marker to identify IAs at risk of rupture.

P 19

A human isogenic in vitro model of the neurovascular unit to explore blood-brain barrier dysfunction in neuroinflammation

P. Kasap[1], M.C. McCloskey[2], S. Perriot[3], R. Du Pasquier[3], J.L. McGrath[2], B. Engelhardt[1], Presenter: P. Kasap[1] ([1]Bern, [2]Rochester, New York, [3]Lausanne)

Objective: The blood-brain barrier (BBB) is established by structurally and biochemically unique brain microvascular endothelial cells (BMECs) that acquire and maintain their characteristics by continuous crosstalk with pericytes and astrocytes. BBB breakdown and immune cell infiltration into the central nervous system (CNS) are amongst the earliest pathological hallmarks of multiple sclerosis (MS). MS is considered a prototypic T cell-mediated autoimmune disease targeting the CNS. However, the mechanisms leading to BBB breakdown and how BBB dysfunction contributes to disease pathogenesis are incompletely understood due to the lack of appropriate tissue samples or patient-derived in vitro BBB models. To this end, we made use of the recent advancements in human-induced pluripotent stem cell (hiPSC) technology to build fully isogenic models of the human neurovascular unit (hNVU) on a chip in which all cell types are sourced from one individual.

Methods: We have built a modular µSiM platform that features ultrathin, transparent, and permeable silicon nitride membranes creating a "blood compartment"lined with hiPSC-derived BMECs and a "brain compartment"harboring hiPSC-derived pericytes and astrocytes. The modular µSiM device enables rapid assembly, use of different membranes with variable pore sizes, and incorporation of modules converting it to a microfluidic, tricellular culturing, or a TEER measurement device.

Results: We employed our recently established extended endothelial cell culture (EECM) method to differentiate hiPSC-derived EECM-BMEC-like cells that develop barrier properties resembling exactly those of primary human BMECs. EECM-BMEC-like cells cultured in the µSiM device formed a monolayer with mature tight junctions, developed barrier properties, and showed cytokine-induced expression of adhesion molecules exactly as previously found when EECM-BMEC-like cells cultured on TranswellTM filter inserts. Furthermore, we successfully cultured hiPSC-derived EECM-BMEC-like cells, pericytes and astrocytes from the same individuum in the µSiM device forming an isogenic neurovascular unit.

Conclusion: Overall, we confirmed the suitability of the µSiM device to study the function of the hNVU in health and neuroinflammation. The addition of a physiological flow unit will finally allow us to investigate immune cell trafficking across the BBB in a fully autologous manner.

P 20

Panx1 as a new target in the prevention of cardiac ischemia/reperfusion injury

O.M. Rusiecka, F. Molica, A. Tollance, S. Morel, M. Frieden, M. Chanson, B.R. Kwak, Presenter: O.M. Rusiecka (Geneva)

Objective: Reperfusion following myocardial ischemia (I/R) is crucial to avoid tissue necrosis, but may result in additional damage. I/R activates endothelial cells leading to ATP release through Pannexin1 (Panx1) channels. ATP acts as a'find me'signal for leukocytes. Here, we investigated the role of Panx1 in cardiac I/R.
Methods: Panx1 expression and channel function were detected by immunofluorescence, Western blot and ATP release assays. Cardiac function was measured ex vivo in Langendorff-perfused hearts from WT or Panx1-/- mice subjected to I/R with or without ischemic pre-conditioning (IPC). In vivo I/R was induced by left coronary artery occlusion in WT, Panx1-/- mice, mice with neutrophil-specific Panx1 deletion (Panx1Ndel) and Panx1fl/fl mice. Mitochondrial membrane potential was imaged with TRME and the oxygen consumption rate was measured by Seahorse.
Results: Panx1 was found in cardiac endothelium, neutrophils and cardiomyocytes. After in vivo I/R, Troponin-I and infarct size were decreased in Panx1-/- mice. Neutrophil infiltration in the infarct was not altered in Panx1-/- mice. Moreover, Troponin-I and infarct size were similar in Panx1Ndel and Panx1fl/fl mice, suggesting that cardioprotection in Panx1-/- mice rather involved cardiomyocytes than the inflammatory response. Panx1 deletion did not affect physiological cardiac function. However, Panx1-/- hearts showed a better recovery of myocardial function after I/R. Time to onset of contracture and to maximal contracture were delayed in Panx1-/- hearts. This improved cardiac recovery was abolished in Panx1-/- hearts subjected to IPC prior to I/R, suggesting an altered mitochondrial function in Panx1-/- cardiomyocytes. Panx1 was found in cardiac mitochondria, where it regulated the ATP content and membrane potential. Finally, Panx1 co- immunoprecipitated with VDAC1 and reduced Panx1 expression lowered basal and maximal mitochondrial respiration.
Conclusion: Panx1-/- mice display decreased sensitivity to cardiac I/R, resulting in smaller infarcts and improved recovery of cardiac function. These cardioprotective effects were independent of neutrophil recruitment but rather relied on the interaction of Panx1 with VDAC1 in cardiac mitochondria. Thus, Panx1 may represent a new cardioprotective target in I/R.

P 21

Vitamin D regulates T-cell migration across the blood-brain barrier

S. Soldati[1], A. Baer[1], A. Pal[1], M. Vladymyrov[1], E. Bouillet[1], F. Gosselet[2], E. Thouvenot[3], A. Astier[4], B. Engelhardt[1], Presenter: S. Soldati[1] ([1]Bern, [2]Lens, [3]Montpellier, [4]Toulouse)

Objective: There is emerging evidence that vitamin D (VitD) plays an important role in the pathogenesis of multiple sclerosis (MS). VitD was shown to decrease the severity of experimental autoimmune encephalomyelitis (EAE), an animal model of MS, by reducing lymphocyte recruitment to the central nervous system. Here we explored if VitD affects the migration of different T-cell subsets across the blood-brain barrier (BBB) in the context of neuroinflammation.
Methods: We first relied on flow cytometry to investigate the effect of VitD on the surface expression of adhesion molecules of human peripheral blood CD4+ and CD8+ T cells and assessed their ability to interact with different recombinant BBB adhesion molecules under static and physiological flow condition in vitro. Secondly, we studied the migration of VitD treated T cells across the BBB under physiological flow condition, by employing a human CD34+ cord-blood stem-cell derived BBB model in vitro, and in mice suffering from active EAE by means of two-photon microscopy.
Results: VitD treatment decreased the surface expression of α4- and αL-integrins on human peripheral blood CD4+ and CD8+ T cells and reduced their adhesion to recombinant VCAM-1 and ICAM-1 under static and physiological flow condition in vitro. Furthermore, VitD treatment decreased T-cell arrest on the BBB endothelium under physiological flow condition in vitro and in vivo, leading also to reduced T-cell diapedesis across the BBB in vitro.
Conclusion: Our results show that VitD regulates the expression of adhesion molecules on human T cells and thus influences their interaction with the BBB. Beneficial effects of VitD in MS may thus be due to reducing T-cell migration across the BBB.

P 22

Novel bioengineered models of a vessel and the perivascular niche for basic research and personalized medicine

B. Dasen, M.G. Muraro, A. Mainardi, G.M. Born, I. Martin, M. Filippova, Presenter: M. Filippova (Basel)

Objective: Personalized medicine is a rapidly developing therapeutic approach aimed at application of individually tailored treatments according to the unique molecular characteristics of a patient. The implementation of personalized treatments into clinical practice is often hindered by the absence of ex vivo models which allow fast and reproducible assessment of patients' samples, analysis of drug sensitivity, and functional validation of genomic data under conditions closely reflecting molecular and cellular events in vivo. AIM: To develop novel bioengineered vessel-on-a-chip models of a microvessel and the bone perivascular niche for the purposes of basic research and personalized medicine.
Methods: Two novel models are based on (1) perfusion bioreactor and (2) a custom microchannel slide. The device hardware was manufactured on 3D printed wafers. Microtissues emulating 3D multicellular structure of the vessel and the bone perivascular niche were constructed from vascular endothelial cells (HUVEC), pericytes, MSC-derived MSOD-BMP2 cell line subjected to osteogenic differentiation, and collagen-based hydrogels mimicking the extracellular matrix. Prostate tumor cell line DU145 was used to emulate circulating cell recruitment to the vascular wall.
Results: The models were characterized by computer simulations with respect to flow and shear stress parameters. The applicability of the assays for the modeling of pathophysiological processes in the perivascular niche was demonstrated by pilot studies on the role for

adhesion molecule T-cadherin in regulation of sprouting angiogenesis, and effects of pro- and anti-inflammatory agents (LPS, TNFalpha, oxidized phospholipids) on metastatic tumor cell extravasation into the vessel wall.
Conclusion: The novel models allow analysis of complex intercellular interactions in the perivascular niche under conditions closely emulating pathophysiological processes in vivo. The study contributes towards the development of novel technologies for personalized drug screening and identification of novel therapeutic molecular targets to treat vascular diseases and cancer. Our design eliminates irreproducibility issues and complex manufacturing procedures typical for microfluidic platforms and may represent an attractive off-the-shelf solution for cell biologists with no experience in bioengineering.

P 23

Apolipoprotein E defines high-density lipoprotein trafficking in brain endothelial cells

S. Kakava, E. Schlumpf, A. von Eckardstein, J. Robert, Presenter: S. Kakava (Zürich)

Objective: Alzheimer's disease (AD) is the leading cause of senile dementia with over 50 million affected individuals worldwide. Its well-known neuropathological hallmarks, beta-amyloid and tangles, are preceded by cerebrovascular damage. High-density lipoprotein (HDL), possesses several vasoprotective functions and epidemiological studies showed associations of very low and very high HDL-cholesterol levels with the risk of AD. Several lines of evidence suggest that HDL reduces AD risk by decreasing both beta-amyloid deposition within the vasculature and vascular inflammation. We previously found that HDL enriched in apolipoprotein (apo)E (HDLE+) are more effective in removing vascular beta-amyloid deposits than those lacking apoE (HDLE-). However, HDL circulating in the blood must first interact with brain endothelial cells (EC) to display its anti-AD properties, a process that is poorly understood.
Methods: HDL was isolated from plasma of healthy donors by ultracentrifugation before being further fractionated into HDLE+ and HDLE by the use of apoE immunoaffinity chromatography -. Fluorescent or 125I- radio labeled HDL were used to measure binding (40C), association, internalization or transport (370C) through primary human brain EC or the cell line hCMEC/D3.
Results: Both HDLE+ and HDLE- were specifically bound, internalized, and transcytosed through brain EC. However upon fluorescence microscopy, they were found only partially co-localized with each other suggesting independent trafficking pathways. Using RNA interference and pharmacological inhibitions, we showed that HDL binding and association were dependent of scavenger receptor BI (SR-BI) and endothelial lipase whereas ATP binding cassette G1 (ABCG1) knockdown only reduced HDL association. Interestingly we found that interference of the low-density lipoprotein receptor (LDLR) also reduced HDL internalization but not binding to brain endothelial cells.
Conclusion: Together our findings suggest distinct trafficking pathways for HDLE+ and HDLE- through brain EC's that might imply different cerebrovascular functions relevant to AD.

P 24

De novo expression of an immunomodulatory molecule on the endothelium controls tumor growth and metastasis

E. Biglieri[1], S. Rotter[1], M. van Gogh[1], J.F. Glaus Garzon[1], I. Jurisica[2], L. Borsig[1], Presenter: S. Rotter[1] ([1]Zürich, [2]Toronto)

Objective: Metastasis is primarily responsible for the morbidity and mortality of cancer. While the process of metastasis is still insufficiently understood and effective treatments are scarce, it is clear that the endothelium is significantly involved in several steps of metastasis. However, the precise role of endothelial cells (ECs) in organ specific metastasis remains poorly understood. Overall, our aim is to study the contribution of the microvascular endothelium to cancer metastasis and identify endothelial derived factors which are essential for the formation of liver and lung metastasis.
Methods: We analyzed RNA transcriptomes of activated ECs from metastatic foci at two different sites (lung and liver), using three different spontaneous metastatic mouse models. Common pathways involved in lung and liver EC activation were analyzed and protein-protein interaction networks identified targets which are highly upregulated and interconnected in ECs of metastatic origin, compared to naïve ECs. We established a mouse model with an EC-specific deficiency of our protein of interest and investigated its impact on lung metastasis.
Results: We identified a member of the TNF receptor family to be specifically upregulated on ECs within metastatic foci, while no expression was detected on ECs in adjacent lung tissue. This inducible co-stimulatory receptor plays a critical role in T cell immune response. However, its role in ECs remains undefined. EC-specific deletion of this receptor resulted in enhanced primary tumor growth and spontaneous lung metastasis, which were associated with changes in the immune microenvironment.
Conclusion: Overall, our study discovered a novel endothelial cell-derived factor which is significantly involved in lung metastasis. We are now in the process of confirming this phenotype in another mouse model and are trying to identify the underlying mechanism. Furthermore, we are studying the different effects of T cell specific and EC specific expression of the receptor in cancer metastasis.

P 25

Activating Anti-TREM2 agonist treatment as a potential therapy for primary familial brain calcification

S. Sridhar[1], A. Ibrahim[2], I. Tassi[2], A. Keller[1], Presenter: S. Sridhar[1] ([1]Zürich, [2]South San Francisco, California)

Objective: Primary familial brain calcification (PFBC) is a brain disease diagnosed by the absence of other common neurodegenerative disorders and the presence of bilateral calcifications in the basal ganglia. Patients of PFBC experience a range of symptoms, ranging from mood disturbances to motor problems and dementia. As such only symptomatic treatments exist for PFBC. Recent data has shown that microglia, the brain resident macrophages, are required to curtail the growth of small vessel associated calcifications in the Pdgfb(ret/

ret) model of PFBC. Microglia require functional Triggering receptor expressed in Myeloid cells 2 (TREM2) for this role. Here we investigated if activating TREM2 signaling in Pdgfb(ret/ret) mice would aid in reducing calcification load and work as a potential therapy route for PFBC patients.

Methods: Two-month-old mice were injected with 60 mg/kg (i.p.) of activating Anti-TREM2 agonist or Control IgG antibody for 8 weeks. A week after the last dose, brains from these mice were dissected and used for biochemistry and histology. Regions with least variability in calcification load were used to quantify calcification number and area. The microglial response to calcifications and extent of TREM2 signaling activation after treatment was also characterized.

Results: The current treatment strategy did not alter calcification load as measured either by number or area. Microglia surrounding calcifications termed as calcification associated microglia did not change their phenotype upon anti-TREM2 antibody treatment. However, anti-TREM2 treatment resulted in uniform deposition of Cathepsin K (collagen I degrading enzyme secreted by microglia on to calcifications) compared to control.

Conclusion: The treatment regimen utilized in the pilot study did not alter calcification load. However, these mice have a significant blood brain barrier breach phenotype and therefore, received nearly 60–100 times more anti- TREM2 antibody than in previously published mouse models. A different regimen is needed to ensure optimal activation of TREM2 signaling in these mice. The pilot study also provided insights regarding the use of Pdgfb(ret/ret) mice for preclinical studies of PFBC. Further studies are required to verify if activating anti-TREM2 antibody can be used to reduce calcification loads and eventually as a treatment for PFBC patients.

P 26

Framework for automated analysis of leukocyte interactions with an in vitro model of the blood-brain barrier under physiological flow

M. Vladymyrov[1], A. Aeschbach[1], S. Aydin[1], L. Marchetti[1], E. Palm[1], S. Perret-Gentil[1], S. Soldati[1], A. Ariga[1,2], B. Engelhardt[1], Presenter: M. Vladymyrov[1] ([1]Bern, [2]Chiba)

Objective: The endothelial blood-brain barrier (BBB) rigorously controls T-cell trafficking into the central nervous system (CNS). Mouse and human-derived brain microvascular endothelial cells (BMECs) in microfluidic devices are powerful in vitro models of the BBB allowing to study the multi-step T-cell extravasation across the BBB under physiological flow by live cell imaging using phase contrast microscopy. Previously available automated tools are not able to reliably differentiate T cells on top of the BMEC monolayers in the grayscale time-lapse datasets obtained in this modality and perform tracking under flow, demanding primarily manual analysis. Here we present our framework allowing for studies of multi-step leukocyte migration cascade under flow. We demonstrate its performance on assays of T-cell migration across the BMEC monolayers under flow in vitro.

Methods: It relies on Convolutional Neural Network based segmentation of T cells moving on top and across the BMEC monolayer and a custom tracking algorithm allowing for T-cell tracking under flow. The pipeline enables scalability and allows for performing cell-by-cell based analysis for each step of the migration cascade. We then employ representation learning techniques to investigate distinct behavioral patterns of T cells and local properties of the BMECs, based on the imaging data.

Results: We demonstrate the performance of the pipeline based on the analysis of a set of assays on CD4 and CD8 T cell migration under flow. We further present the first results of the local BMEC properties effect on T cell migration.

Conclusion: Our developed framework enables automated scalable investigation of T cell migration across the in vitro BBB model in an unbiased way. It enables gaining more insight on the behavior of individual T cells and their interaction with individual endothelial cells. It will serve as foundation for studies of interactions of other immune cell subsets with endothelial or epithelial monolayers. This will allow us to unravel the cellular and molecular cues promoting immune cell infiltration into the CNS in vitro.

P 27

Identification of brain vascular cell-cell interactome: Pericyte heterogeneity

S.-F. Huang, A. Keller, Presenter: S.-F. Huang (Zürich)

Objective: Dysregulated cell-cell communication at the neurovascular unit (NVU) leads to a vascular dysfunction and is associated with many neurological disorders. The cerebral vasculature is heterogeneous with distinct zones -arterial, capillary, venous – formed by specific cell types. It is likely that the cell-cell communication at the NVU differs along the vascular tree during physiology and diseases. However, an understanding how vascular cells interact with each other is poor. Here, we aim to establish a comprehensive cell-cell interactome along the cerebral vasculature.

Methods: We are "cataloguing" potential paracrine and autocrine cell-cell interactions, and-cell-matrix interactions at the NVU using publicly available single-cell/nuclei RNAseq datasets and NATMI (Network Analysis Toolkit for Multicellular Interactions) and Cellchat algorithm. We explored a mouse brain vascular single-cell dataset that has 10 distinct vascular associated cell types. Pericyte subclusters were identified by Seurat (4.0) package and further validated in C57BL/6 mouse brains by immunofluorescent staining. Images were taken by Leica SP5 confocal laser scanning microscope (Leica microsystems, 20X objective) and analyzed by the image processing software Fiji and Imaris.

Results: The cell-cell interactome showed differences along the arteriovenous axis of the mouse brain dataset. Arteriolar EC ligands mostly communicate with PVFs, whereas venous EC ligands mostly communicate with SMC. The pathway analysis shows similarity between enriched pathways in EC along the arteriovenous axis, although the molecular composition differs. The PC subtypes, Ace2 high and Ace2 low PC, were identified and validated, which showed different in Spp1, Casq2 and Ace2 mRNA and protein expression. We further investigate the distribution of Ace2 high and Ace2 low PC in different brain regions and the associated vessel diameter. Interestingly, Ace2 low PC were more abound in deep brain region. We analyzed the interactome of capillary EC and both PC subtypes, interestingly similar ligand-receptor pairs found in both PC subtypes but with different strength.

Conclusion: The disruption/ imbalance of vascular cell-cell interactions could cause vascular dysfunction. Our in- depth analysis gives insights into the cellular signaling network at the NVU and will serve as a resource aiding the identification of NVU alterations during brain pathology.

P 28

ICAM-1 expression is upregulated in blood and lymphatic vessels during Malassezia infection

J.D. Medina Sanchez[1], M. Tuor[2], S. LeibundGut-Landmann[2], C. Halin[1], Presenter: J.D. Medina Sanchez[1] ([1]Zurich, [2]Zürich)

Objective: Malassezia is the most common fungus on mammalian skin and an important part of the skin microbiome (50–80%). It has been described as commensal, but under certain conditions, e.g. immunosuppression, it can also develop opportunistic infections. VCAM-1 and ICAM-1 are cellular adhesion molecules that play a crucial role for T and DC migration through blood vessels (BVs) and lymphatic vessels (LVs) during inflammation. However, whether ICAM-1 or VCAM-1 upregulation in LVs affects the developing immune response during Malassezia infection has not yet been studied.

Investigate ICAM-1 and VCAM-1 expression during Malassezia infection in endothelial cells (ECs) from infected skin.

Methods: Mouse ears were infected with Malassezia by topical application. On the second day, the ears were collected along with samples from uninfected, vehicle-treated mice (vehicle). As a positive control, inflammation was induced by topical application of the irritant molecule TPA on the ears of mice, samples were collected 24 hours later. As a negative control, steady-state mouse ears were used. The expression of adhesion molecules ICAM-1 and VCAM-1 by ECs was subsequently analyzed in single cell suspensions generated from the different samples.

Results: Our analysis revealed that ICAM-1 was already expressed by ECs in steady-state and in vehicle-treated samples. However, upon TPA-induced inflammation or infection, ICAM-1 expression was significantly upregulated in all types of ECs. On the other hand, ECs poorly expressed VCAM-1 in steady-state and in mock-infected samples. VCAM-1 expression was increased in ECs derived from lymphatic collectors in TPA-inflamed skin, but not during Malassezia infection.

Conclusion: We found ICAM-1 but not VCAM-1 to be strongly upregulated in ECs derived from LVs during Malassezia infection. To investigate the importance of ICAM-1 in leukocyte egress from infected skin and in the overall anti-fungal immunity, we are currently generating a lymphatic-specific conditional ICAM-1 knock-out mouse line. These will allow us to uncouple leukocyte recruitment via blood vessels from leukocyte egress via LVs.

P 29

Imaging leukocyte migration into lymphatics in human skin

L. Zambounis[1], R. Gähwiler[1], E. Gousopoulos[2], G. Restivo[2], M. Levesque[2], N. Lindenblatt[2], C. Halin[1], Presenter: L. Zambounis[1] ([1]Zurich, [2]Zürich)

Objective: In the past 20 years, immune cell migration into lymphatic vessels (LVs) has been studied extensively in the murine setting. However, in the human context, leukocyte migration through afferent lymphatic vessels is still poorly characterized, and it is thus far not completely clear whether all the findings made in the murine setting can be directly translated to the human condition. To overcome this problem, we have recently established an assay to investigate migration of dendritic cells (DCs) into lymphatic vessels in cultured human dermal skin slices cut from surgical biopsies.

Methods: To investigate the migration of DCs into LVs in human skin, we first established the conditions for staining different leukocyte subsets and lymphatic vessels in 3D by confocal microscopy in human skin slices. In the case of DCs, it was previously shown that, upon incubation of human skin, DC start to mature, likely due to recognition of damage-associated molecular patterns (DAMPs), what induces their migration into lymphatic capillaries. To investigate whether this migration could be blocked in presence of potential inhibitors, we incubated the skin in culture medium either in absence or presence of pertussis toxin (PTX). The latter is a well- known inhibitor of Gai-coupled receptors, such as chemokine receptors. As a readout of migration, skin slices were harvested after approx. 46 hours, DCs and LVs stained with fluorescent antibodies and the localization of DCs in the tissue – specifically, the ratio of intralymphatic to interstitial DCs – was quantified by microscopy.

Results: Blinded analysis of the acquired image sets revealed that DCs from human skin slices incubated in control medium successfully entered LVs, while this process was profoundly and significantly reduced in presence of PTX.

Conclusion: We have successfully established a new assay for investigating DC migration into LVs in human skin. In the future, we plan to test the involvement of specific mediators, such as chemokines, sphingosine-1- phosphate or adhesion molecules, in human DC migration. We are further working on establishing time-lapse imaging of DC migration in human skin slices.

P 30

Cerebrospinal fluid outflow pathways at the cribriform plate along the olfactory nerves

I. Spera, S.T. Proulx, Presenter: I. Spera (Bern)

Objective: Several studies have shown that routes along the olfactory nerves that extend to lymphatic vessels in the nasal submucosa are an important cerebrospinal fluid (CSF) outflow pathway. Previous evidence in our lab showed an accumulation of fluorescent tracers at the cribriform plate, indicating the outflow has also occurred along the olfactory nerves. However, it is still unclear how fluid pathways along the nerves connect to the lymphatic vessels and where the arachnoid barrier is breached. This study aims to define anatomically the connections between the subarachnoid space (SAS) and the lymphatic system.

Methods: We made use of Prox1-GFP reporter mice to visualize the lymphatic vessels. To identify the CSF outflow pathways, pegylated (PEG) or unmodified microbeads (2.5 uL of 0.25% v/v in PBS) have been infused intracerebroventricularly in Prox1-GFP mice. At 45 min after the infusion, mice were sacrificed, and a decalcification protocol was used to keep the bone structures of interest intact. Then, 20 um thick slices were obtained at the cryostat, and imaging at the level of the cribriform plate was performed under either a fluorescence stereomicroscope or a confocal microscope. In some samples, we did immunofluorescence staining with an E-cadherin antibody to detect the arachnoid barrier.

Results: As expected, unmodified microbeads remain stuck into the ventricles compared to the pegylated ones. Therefore, they are not ideal for studying the CSF outflow pathways. In the area immediately below the olfactory bulbs, where the olfactory nerves cross the cribriform plate, we observed PEG micro beads around the nerve bundles and into the lymphatic vessels crossing the cribriform plate. In addition, E- Cadherin staining revealed a discontinuous distribution of the arachnoid barrier at the midline under and between the olfactory bulbs.
Conclusion: These data showed that the PEG beads have a better drainage efficiency than unmodified beads. Furthermore, our results indicate that there are direct and open connections from the CSF space to the lymphatic vessels crossing the cribriform plate and in the nasal submucosa, as particles of one-micron diameter had access to the lymphatics. Supporting this conclusion, we did not observe beads in the submucosal interstitial tissue. Finally, the discontinuous distribution of the arachnoid barrier in this area could explain how the lymphatics access the SAS.

P 31

Macrophage-derived Vascular Endothelial Growth Factor is required for adrenal gland homeostasis and blood pressure control

Z. Fan, M. Karakone, J. Loffing, C. Stockmann,
Presenter: Z. Fan (Zürich)

Objective: The aldosterone-producing zona glomerulosa of the adrenal gland cortex is characterized by a high density of sinusoidal blood vessels which are intimately associated with macrophages. However, the function of these adrenal gland harboring macrophages in steady-state conditions remains largely unknown. The preservation of the vascular phenotype is likely to be vital for proper adrenal gland function. In this study, we investigated the role of macrophage-derived Vascular Endothelial Growth Factor A (VEGF-A) in adrenal gland homeostasis, ion balance and blood pressure control.
Methods: Morphological analysis of adrenal gland from myeloid cell-specific VEGF-A knockout mice revealed decreased vascular density specifically in the aldosterone-producing zona glomerulosa. This was associated with subendothelial fibrosis as evidenced by thickening of endothelial basement membrane and increased deposition of the extracellular matrix component collagen I.
Results: Functional analysis showed an increased aldosterone synthase expression in the zona glomerulosa of the adrenal gland from knockout mice along with decreased renin expression in the kidney, high blood pressure, and hypokalemia, strongly reminiscent of primary aldosteronism. Moreover, immunohistochemistry staining performed on human aldosterone-producing adrenal adenomas revealed increased deposition of collagen I and collagen IV.
Conclusion: Taken together, we hypothesize that macrophage-derived VEGF-A is critical for vascular maintenance in the adrenal gland and that perturbations in VEGF signaling are potentially involved in the pathogenesis of aldosteronism and hypertension.

Autorenverzeichnis/Relevé des auteurs